

Y-junction connecting Luttinger liquids: fixed point structure and conductances

D.N. Aristov^{1,2,3} and P. Wölfle^{2,4}

¹*Petersburg Nuclear Physics Institute, Gatchina 188300, Russia*

²*Institute for Nanotechnology, Karlsruhe Institute of Technology, 76021 Karlsruhe, Germany*

³*Department of Physics, St.Petersburg State University,*

Ulianovskaya 1, Petrodvorets, St.Petersburg 198504, Russia

⁴*Institute for Condensed Matter Theory, and Center for Functional Nanostructures,*

Karlsruhe Institute of Technology, 76128 Karlsruhe, Germany

(Dated: June 15, 2018)

We study the transport properties of three Luttinger liquid wires (with possibly different interaction strength), connected through a Y-junction, within the scattering state formalism. We first formulate the problem in current algebra language and focus on the case of a symmetric set-up, for which the scattering matrix and the matrix of conductances is parametrized by two variables. For these we derive coupled RG equations, first in a ladder summation up to infinite order in the interaction. The fixed point structure and the implicit solution of these equations is presented. It is shown that higher order terms beyond the ladder approximation do not change the scaling behavior near the fixed points. For sufficiently strong attractive interaction a new fixed point with unusual properties is found.

I. INTRODUCTION

Electron transport in strictly one-dimensional quantum wires is governed by the Coulomb interaction between electrons. This is spectacularly demonstrated by the fact that within the Tomonaga-Luttinger liquid (TLL) model in the limit of temperature $T \rightarrow 0$ the conductance of a quantum wire with finite barrier tends to zero, provided the interaction is repulsive and assumes the maximum value $G = 1$ (in units of the conductance quantum $G_0 = e^2/h$) for attractive interaction. The latter behavior appears independent of the strength of the scattering at the barrier, and can be traced back to the formation of Friedel oscillations of the charge density around the barrier, leading to an infinitely extended effective barrier potential in that limit.

TLL behavior has recently been studied experimentally in carbon nano-tubes.^{1,2} In a future nanoelectronics constructed out of quantum wires, junctions of three or more wires will necessarily be involved, requiring a knowledge of the fundamental transport behavior of electrons in such structures. It is known that such systems exhibit rather rich TLL effects which have been the subject of a number of recent papers.³⁻¹⁷ Much of the work in this field has used the bosonization method, which gives rise to the problem of how to preserve the fermionic character of charge carriers. When the number of wires meeting at a junction exceeds two, the Klein factors, which give Fermi statistics to the bosonized operators of different wires, are more difficult to handle.³ Oshikawa et al. recently introduced¹⁸ a new method to study this problem, mapping it into the dissipative Hofstadter model (DHM), which describes a single particle moving in a uniform magnetic field and a periodic potential in two dimensions and coupled to a bath of harmonic oscillators. When the three quantum wires enclose a magnetic flux, the mapping to the DHM also allows to identify a new low energy chiral fixed point with an asymmetric

flow of current that is highly sensitive to the sign of the flux. The paper by¹⁸ is giving a systematic and thorough treatment of the three lead junction problem, and we shall refer to it later, when we compare our results with theirs. It should be noted, however, that in spite of their success, the above mentioned methods do not in general allow to determine the fixed point (FP) structure of the theory in an unbiased way, as they require a certain knowledge of the existence of FPs as a starting point.

In this paper we follow a different route: we describe the transport properties in fermionic language, thus avoiding the problem of Klein factors and the necessity to assume the existence of FPs. As shown in our previous work, one may recover the known results on transport through a TLL wire with barrier and obtain new results not accessible by other methods within the fermionic formulation.¹⁹ Moreover, as this method is formulated in a scattering wave picture, the connection of the interacting wire to non-interacting reservoirs is naturally included. While this formulation has previously been regarded as being restricted to weak coupling^{6,20,21} we have shown in an earlier work that it may be extended to the strong coupling regime in a controlled way by using an infinite resummation of perturbation theory (ladder summation). The result obtained in this approximation is universal, i.e. does not depend on the ultraviolet cutoff chosen.

We restrict ourselves to a symmetric time-reversal invariant setup, which is characterized by two independent components of the conductance tensor. This setup in case of one wire without interaction is relevant to the problem of tunneling into a Luttinger liquid and was studied in²² for weak interaction. There it has been found that the asymmetric fixed point A (perfectly conducting wire and a vanishing tunneling amplitude into the tip, see below) becomes unstable in the case of weak repulsive interaction once the description of the Y-junction is not reduced to the simple tunneling model. A further remarkable re-

sult of that work is the finding of a nonmonotonic behavior of the conductance (e.g. as a function of temperature), in certain cases. We extend that work here to arbitrary interaction and find similar behavior at strong interaction.

The resulting coupled RG equations will first be analyzed with respect to their fixed point structure. We find four fixed points, labelled N,A,M,Q, where at N (Neumann) the three wires are totally separated, at A (asymmetric) the third wire is separated, while the main wire is perfectly conducting, at M (mystery) and Q (quaint) the conductances take an intermediate value, depending on the interaction strength. All fixed points are located on the boundary curve marking the allowed area in the plane of the two conductances. For repulsive interaction only N is stable, A being a saddle point. For attractive interaction N is unstable and M is stable. For stronger attractive interaction, beyond a threshold value A becomes an additional stable fixed point. The conductances are calculated analytically for several special cases of interest. We present and discuss the power law exponents appearing in the various regimes.

In order to check the reliability of the ladder summation result, we calculate all scale dependent terms (in the limit of $T = 0$) up to third order in the interaction. We find several terms additional to the ladder terms. These terms are nonuniversal and subleading, in the sense that they disappear for the case of repulsive interaction, when one of the stable fixed points is approached. For attractive interaction, the properties of the new fixed point M appear to be affected by the three-loop terms beyond the ladder approximation.

The paper is organized as follows. In section II we define the model of a Y-junction considered here. We introduce the currents in the SU(3)-representation and define the Hamiltonian in the chiral representation. Section III is devoted to an analysis of the scattering matrix and the derivation of the conductance tensor in terms of the S-matrix components. We consider a simple tunneling case and the totally symmetric case, both characterized by only a single free parameter in the S-matrix and the general Y-junction case with two parameters and therefore two independent conductance components. In section IV we show how the RG equation for the simple tunneling case is extracted from perturbation theory in the ladder approximation, and discuss the ensuing conductance. The RG equation for the general Y-junction case is presented in section IV B. We further present the results on the nonuniversal terms in third order perturbation theory in section V. Finally, the RG phase diagram is presented and discussed in section VI.

II. MODEL OF A Y-JUNCTION

We consider the setup of a Y-junction: a quantum wire of finite length $2L$ connected to noninteracting leads, and a tip with attached wire forming a contact (junction) in

the center of the wire, which for simplicity is assumed to have the same length L , also connected to a noninteracting lead. We choose the origin of the coordinate system at the junction and denote the two halves of the main wire by indices 1 and 2 and the tip by 3. We consider spinless fermions. In the following we will refer to the so defined symmetric (leads 1, 2) set up as a Y-junction. A particularly simple version to be considered below is a simple tunneling junction (no tunneling barriers, only on site tunneling). Below we will also briefly consider a totally symmetric junction (with respect to interchanging any pair of wires).

The electrons are assumed to interact via a short-ranged interaction of arbitrary strength and sign between incoming and outgoing fermions. In the present case, instead of defining right- and left-movers, it is more appropriate to speak of incoming and outgoing waves, with respect to the junction, or “origin”.

The short-range interaction is characterized by the amplitude g in the main wire (1 and 2) and a different amplitude g_3 in the third wire. This interaction takes place at $x < L$, measuring from the origin. In order to spatially separate effects of the potential scattering at the origin and the interaction, we also assume that the interaction takes place at $x > a_0$, whereas the potential scattering happens at $x < a_0$. The scale a_0 appears below as short-range cutoff of the theory.

The Hamiltonian of the system is

$$\mathcal{H} = \int_{-\infty}^0 dx \sum_{j=1}^3 H_j \quad (1)$$

$$H_j = v_F \psi_{j,in}^\dagger i \nabla \psi_{j,in} - v_F \psi_{j,out}^\dagger i \nabla \psi_{j,out} + 2\pi v_F g_j \psi_{j,in}^\dagger \psi_{j,in} \psi_{j,out}^\dagger \psi_{j,out} \quad (2)$$

where we did not write explicitly the range function of the interaction. In the chosen parametrization the amplitudes g_j are dimensionless and enter the subsequent expressions in the most convenient form.

We unfold the setup in the usual way,^{23,24} by putting the incoming fermions on the negative x -axis and the fermions, which have passed through the junction, at positive $|x|$. As a result, we have a three-fold multiplet of right-going fermions with non-local interaction. This procedure is depicted in Fig. 1

The boundary condition at the origin is described by the scattering S-matrix as follows. For elastic scattering by the central dot, the outgoing fermions at the origin are connected to the incoming ones by the relation $\psi_{k,out}^\dagger = S_{km}^* \psi_{m,in}^\dagger$. We choose S in the symmetric way as described at length in the next subsection.

In the scattered states representation, the right- and left-going fermionic densities acquire the form

$$\begin{aligned} \psi_{j,in}(x) &= \psi_j(x), & \psi_{j,out}(x) &= (S \cdot \psi)_j(-x) \\ \psi_{j,in}^\dagger(x) \psi_{j,in}(x) &= \rho_j(x), & \psi_{j,out}^\dagger(x) \psi_{j,out}(x) &= \tilde{\rho}_j(-x) \end{aligned} \quad (3)$$

here and below we use the notation $\tilde{A} = S^\dagger \cdot A \cdot S$.

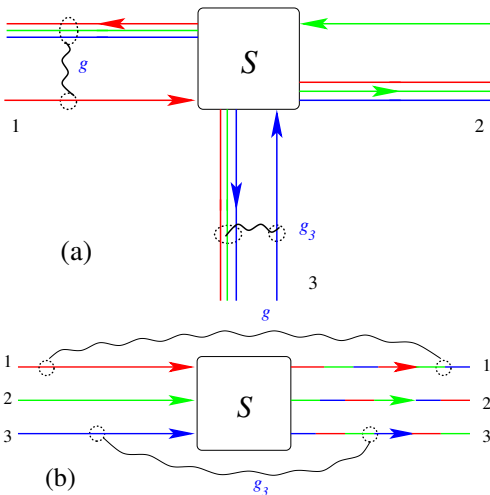


FIG. 1: (Color online) (a) The geometry of a Y-junction is shown together with currents of incoming and outgoing fermions, the type of fermions in the scattered states representation is indicated by its color. The local short-range interaction between the fermions is shown by a wavy line. (b) The equivalent representation in the chiral fermion basis after the unfolding procedure; the initially local interaction becomes non-local, as described by Eq. (8).

Let us explain the meaning of these quantities. We introduce a multiplet of incoming fermions $\Psi = (\psi_1, \psi_2, \psi_3)$. The incoming density $\rho_j = \Psi^\dagger \cdot \hat{\rho}_j \cdot \Psi$ is given by a diagonal matrix, i.e.

$$\begin{aligned} \hat{\rho}_1 &= \begin{pmatrix} 1 & 0 & 0 \\ 0 & 0 & 0 \\ 0 & 0 & 0 \end{pmatrix} = \frac{1}{2} \left(\sqrt{\frac{2}{3}} \lambda_0 + \frac{1}{\sqrt{3}} \lambda_8 + \lambda_3 \right) \\ \hat{\rho}_2 &= \begin{pmatrix} 0 & 0 & 0 \\ 0 & 1 & 0 \\ 0 & 0 & 0 \end{pmatrix} = \frac{1}{2} \left(\sqrt{\frac{2}{3}} \lambda_0 + \frac{1}{\sqrt{3}} \lambda_8 - \lambda_3 \right) \\ \hat{\rho}_3 &= \begin{pmatrix} 0 & 0 & 0 \\ 0 & 0 & 0 \\ 0 & 0 & 1 \end{pmatrix} = \frac{1}{\sqrt{6}} \lambda_0 - \frac{1}{\sqrt{3}} \lambda_8 \end{aligned} \quad (4)$$

Here and below λ_j , with $j = 1, \dots, 8$ are the traceless Gell-Mann matrices, discussed in the Appendix A. In addition to these, we use also the matrix $\lambda_0 = \sqrt{\frac{2}{3}} \mathbf{1}$, which is proportional to the unit matrix, $\mathbf{1}$.

The outgoing densities are given by $\tilde{\rho}_j = \delta_{jk} S_{kl}^* S_{km} \psi_l^\dagger \psi_m = \Psi^\dagger \cdot S^\dagger \cdot \hat{\rho}_j \cdot S \cdot \Psi$, so that in the matrix representation $\hat{\tilde{\rho}}_j = S^\dagger \cdot \hat{\rho}_j \cdot S$. We will mostly omit the hat sign over ρ below.

In terms of the above densities the interaction terms

may now be written.

$$\begin{aligned} &\rho_1(-x) \tilde{\rho}_1(x) + \rho_2(-x) \tilde{\rho}_2(x) \\ &= \frac{1}{2} \Psi^\dagger(-x) \left(\sqrt{\frac{2}{3}} \lambda_0 + \frac{1}{\sqrt{3}} \lambda_8 \right) \Psi(-x) \\ &\times \Psi^\dagger(x) \left(\sqrt{\frac{2}{3}} \lambda_0 + \frac{1}{\sqrt{3}} \tilde{\lambda}_8 \right) \Psi(x) \\ &+ \frac{1}{2} \Psi^\dagger(-x) \lambda_3 \Psi(-x) \Psi^\dagger(x) \tilde{\lambda}_3 \Psi(x) \end{aligned} \quad (5)$$

where $\tilde{\lambda}_j = S^\dagger \cdot \lambda_j \cdot S$, or simply

$$\begin{aligned} \rho_1 \tilde{\rho}_1 + \rho_2 \tilde{\rho}_2 &= \left[\frac{1}{\sqrt{3}} \lambda_0 + \frac{1}{\sqrt{6}} \lambda_8 \right] \left[\frac{1}{\sqrt{3}} \lambda_0 + \frac{1}{\sqrt{6}} \tilde{\lambda}_8 \right] \\ &+ \frac{1}{2} \lambda_3 \tilde{\lambda}_3 \equiv \rho_+ \tilde{\rho}_+ + \rho_- \tilde{\rho}_- \end{aligned} \quad (6)$$

$$\rho_3 \tilde{\rho}_3 = \left(\frac{1}{\sqrt{6}} \lambda_0 - \frac{1}{\sqrt{3}} \lambda_8 \right) \left(\frac{1}{\sqrt{6}} \lambda_0 - \frac{1}{\sqrt{3}} \tilde{\lambda}_8 \right) \quad (7)$$

Here we defined $\rho_+ = \frac{1}{\sqrt{3}} \lambda_0 + \frac{1}{\sqrt{6}} \lambda_8$, $\rho_3 = \frac{1}{\sqrt{6}} \lambda_0 - \frac{1}{\sqrt{3}} \lambda_8$, and $\rho_- = \frac{1}{\sqrt{2}} \lambda_3$.

In terms of these quantities, the Hamiltonian takes the following form (from now on we set $v_F = 1$)

$$\begin{aligned} \mathcal{H} &= \int_{-\infty}^{\infty} dx \left[\sum_{j=1, \dots, 3} \psi_j^\dagger i \nabla \psi_j \right. \\ &\left. + 2\pi \Theta(a < x < L) (g \rho_+ \tilde{\rho}_+ + g \rho_- \tilde{\rho}_- + g_3 \rho_3 \tilde{\rho}_3) \right] \end{aligned} \quad (8)$$

where ρ_\pm, ρ_3 refer to $-x$ and $\tilde{\rho}_\pm, \tilde{\rho}_3$ refer to x , and $\Theta(a < x < L)$ is equal to 1 within the interval specified and zero elsewhere.

For simplicity we do not consider here the so-called g_4 part of the fermionic interaction, i.e. the terms $\pi v_F \tilde{g}_j [(\psi_{j,in}^\dagger \psi_{j,in})^2 + (\psi_{j,out}^\dagger \psi_{j,out})^2]$. It is known that the g_4 -interaction can be absorbed into the redefinition of the group velocity inside the interacting region, $\tilde{v}_{Fj} = v_F(1 + \tilde{g}_j)$. For finite L one can show that g_4 does not lead to a renormalization of d.c. conductance, which is the quantity of our interest below. The effect of g_4 on the a.c. conductance can be analyzed, e.g., following the guidelines in²⁵.

III. S-MATRIX AND CONDUCTANCES

A. S-matrix

The most general S-matrix is defined as follows

$$S = \begin{pmatrix} r_1 & t_{12} & t_{13} \\ t_{21} & r_2 & t_{23} \\ t_{31} & t_{32} & r_3 \end{pmatrix} \quad (9)$$

where r_j is the reflection amplitude for wire j , and t_{jk} is the transmission amplitude between wires j and k . The

matrix S is unitary $S^\dagger S = 1$, which allows its parameterization via the exponential, $S = \exp\left(i \sum_{j=0}^8 \theta_j \lambda_j\right)$. Obviously, there is a redundancy in the description by the nine real-valued parameters θ_j in the exponent, as only the densities and not the fermion amplitudes enter the observables.

The number of physically relevant parameters for the description of the S -matrix may be determined as follows. One may fix the relative $U(1)$ phase between the ingoing and outgoing electrons in each wire, by demanding that the reflection coefficients are real valued. This excludes the λ_3 and λ_8 components. It turns out that it is more convenient to keep the λ_8 component, at the cost of introducing some redundancy, see below. In addition the overall phase described by the λ_0 term may be set to zero.

A further reduction in the number of independent parameters may be derived from the following consideration. In the limit of three almost detached wires, we have $S \simeq \mathbb{1} + i \sum_{j=0}^8 \theta_j \lambda_j$, and $\theta_j \ll 1$. This limiting case elucidates the meaning of the θ_j as the tunneling amplitudes between the corresponding wires. For example, the infinitesimal hopping between wires 1 and 3 of the form $(t_{13} \psi_3^\dagger \psi_1 + h.c.)|_{x=0}$ leads to $\theta_4 = \text{Re}(t_{13})/v_F$, $\theta_5 = \text{Im}(t_{13})/v_F$ with v_F the Fermi velocity, cf.¹⁸. It should be noted that this correspondence between the Hamiltonian and the S -matrix holds only in the limiting cases, and starts to depend on the definition of the regularization procedure in higher orders of t_{kl} , i.e. beyond the Born approximation.¹⁹

By using the above correspondence of the (small) θ_j and the tunneling amplitudes it becomes clear that without loss of generality one may require real-valued hopping amplitudes t_{13} and t_{23} , i.e. coinciding phases for hopping from the third wire into wires 1 or 2 (in the absence of magnetic flux). This makes $\theta_5 = \theta_7 = 0$. After that the phase of the complex valued amplitude t_{12} between the wires 1 and 2 is fixed. In the absence of magnetic fields it must be zero¹⁸ anyway, which further reduces the number of components, since it requires $\theta_2 = 0$.

Thus in the time-reversal invariant situation, the S -matrix can be parametrized by three angles, $\theta_1, \theta_4, \theta_6$. In the presence of a magnetic field a fourth component, θ_2 , appears. We do not consider this case here.

In this paper we concentrate on the case of tunneling into the center of a Luttinger liquid wire. This amounts to full symmetry between the wires 1 and 2, and it reduces the number of independent parameters further to only two, θ_1 and $\theta_4 = \theta_6$.

As mentioned above, we will in addition keep the angle θ_8 . The reason for the introduction of the λ_8 component is two-fold. First, the explicit analytic expressions for S below are somewhat simplified. Second, even if we choose to start without λ_8 component, it will be generated during the renormalization process, as we show below in Sec. IV B. This means that the three angles θ_j , $j = 1, 4, 8$, are not independent. Below we will identify proper combi-

nations of these variables forming a minimal set of two independent variables, in terms of which all the other quantities may be expressed. We then parametrize the three angles in terms of a set of new angles $\tilde{\theta}, \tilde{\phi}, \tilde{\psi}$ as follows

$$\sum_{j=1}^8 \theta_j \lambda_j = \tilde{\theta} \cos \phi (\lambda_4 + \lambda_6) / \sqrt{2} + \frac{1}{2} (\tilde{\theta} \sin \phi + \tilde{\psi}) \lambda_1 + \frac{1}{2\sqrt{3}} (3\tilde{\theta} \sin \phi - \tilde{\psi}) \lambda_8 \quad (10)$$

Explicitly we have the representation of the S -matrix in terms of three angles $\tilde{\theta}, \tilde{\phi}, \tilde{\psi}$

$$S = e^{i\tilde{\psi}/3} \begin{pmatrix} r_1 & t_1 & t_2 \\ t_1 & r_1 & t_2 \\ t_2 & t_2 & r_2 \end{pmatrix} \quad (11)$$

with

$$\begin{aligned} r_1 &= \frac{1}{2} (e^{-i\tilde{\psi}} + \cos \tilde{\theta} + i \sin \tilde{\theta} \sin \phi) \\ t_1 &= \frac{1}{2} (-e^{-i\tilde{\psi}} + \cos \tilde{\theta} + i \sin \tilde{\theta} \sin \phi) \\ t_2 &= \frac{i}{\sqrt{2}} \sin \tilde{\theta} \cos \phi \\ r_2 &= \cos \tilde{\theta} - i \sin \tilde{\theta} \sin \phi \end{aligned} \quad (12)$$

To identify one of the variables as redundant, we use the transformation $(\tilde{\theta}, \tilde{\phi}, \tilde{\psi}) \rightarrow (\theta, \psi, \gamma)$, with

$$\begin{aligned} \tan \gamma &= \sin \phi \tan \tilde{\theta}, \quad \psi = \tilde{\psi} + \gamma, \\ \cos \theta &= \frac{\cos \tilde{\theta}}{\cos \gamma}. \end{aligned} \quad (13)$$

After some calculation we find the components of the S -matrix (up to an overall phase factor $e^{i(\psi-\gamma)/3}$) as

$$\begin{aligned} r_1 &= \frac{1}{2} (e^{-i\psi} + \cos \theta) e^{i\gamma} \\ t_1 &= \frac{1}{2} (-e^{-i\psi} + \cos \theta) e^{i\gamma} \\ t_2 &= \frac{i}{\sqrt{2}} \sin \theta \\ r_2 &= \cos \theta e^{-i\gamma} \end{aligned} \quad (14)$$

We show in the next subsection that the new third variable γ does not appear in any of the components of the conductance. In addition, we will see later in Sec. IV B that γ does not take part in the renormalization process.

It will turn out to be useful to consider the most elementary case of tunneling from the third wire into the main wire (no next neighbor tunneling or tunneling barrier) separately. In that case the S -matrix is characterized by a single angle, $\theta = \sqrt{2}\theta_4 = \sqrt{2}\theta_6$, whereas $\theta_1 = 0$. In terms of the above variables we have $(\tilde{\theta}, \tilde{\phi}, \tilde{\psi}) = (\theta, 0, 0)$ or else $(\theta, \psi, \gamma) = (\theta, 0, 0)$.

In the fully symmetric case of a junction of three identical wires (identical interaction strength and reflection coefficients) we have only one independent angle

characterizing the S-matrix, $\theta = \theta_1 = \theta_4 = \theta_6$. The connection to the above $(\theta, \phi, \tilde{\psi})$, (θ, ψ, γ) is not very transparent, and up to an overall phase factor we have $r_1 = r_2 = (2 + e^{3i\theta})/3$, $t_1 = t_2 = (-1 + e^{3i\theta})/3$.

B. Conductances

The observables we concentrate on in this work are the linear conductances. We first discuss the question of the number of independent linear conductances. The matrix of conductances, G_{jk} , is defined through the relation connecting the current I_j in a given wire with the electric potentials V_k in all the leads as $I_j = \sum_k G_{jk} V_k$. The current in the j th wire is given by $I_j(x) = ev_F(\langle \rho_{j,in}(x) \rangle - \langle \rho_{j,out}(-x) \rangle)$. The electric potentials V_k give rise to the following source term in the Hamiltonian, $H_V = e \int_{-\infty}^0 dx \sum_k V_k (\rho_{k,in}(x) + \rho_{k,out}(-x))$. In linear response theory¹⁹ the currents are given by $I_j(x) = \int_{-\infty}^0 dy (\langle \rho_j(x) \rho_k(y) \rangle - \langle \tilde{\rho}_j(-x) \rho_k(y) \rangle) V_k$. In the static limit and in the absence of interaction the response functions may be evaluated to give

$$G_{jk} = \delta_{jk} - Tr(\hat{\rho}_j \hat{\rho}_k) = \delta_{jk} - |S_{jk}|^2 \quad (15)$$

One easily verifies that the charge is conserved, $\sum_j G_{jk} = 0$, and that applying equal potentials to all wires produces no current, $\sum_k G_{jk} = 0$.

In view of these conservation laws, it is more instructive to discuss the current response to certain bias voltages. Let us define $(I_a, I_b, I_0) = \hat{G} \cdot (V_a, V_b, V_0)$, with

$$\begin{aligned} V_a &= (V_1 - V_2), & I_a &= (I_1 - I_2)/2, \\ V_b &= (V_1 + V_2 - 2V_3)/2, & I_b &= (I_1 + I_2 - 2I_3)/3, \\ V_0 &= (V_1 + V_2 + V_3)/3, & I_0 &= (I_1 + I_2 + I_3)/3, \end{aligned} \quad (16)$$

In this notation, we seek the retarded response of the current $I_a(x) = \frac{1}{2} ev_F (\langle \psi^\dagger \lambda_3 \psi(x) \rangle - \langle \psi^\dagger \tilde{\lambda}_3 \psi(-x) \rangle)$, to the source term, e.g., $H_{V,a} = \frac{e}{2} \int_{-\infty}^0 dx V_a \psi^\dagger \lambda_3 \psi(x)$. We can write these combinations symbolically in the static limit as

$$\begin{aligned} H_V &= \frac{1}{2} V_a \lambda_3 + \frac{1}{\sqrt{3}} V_b \lambda_8 + \frac{1}{\sqrt{6}} V_0 \lambda_0, \\ I_a &= \frac{1}{2} (\lambda_3 - \tilde{\lambda}_3), & I_b &= \frac{1}{\sqrt{3}} (\lambda_8 - \tilde{\lambda}_8), \\ I_0 &= \frac{1}{\sqrt{6}} (\lambda_0 - \tilde{\lambda}_0) \rightarrow 0, \end{aligned} \quad (17)$$

As expected, $I_0 = 0$; in addition we may choose the zero of the electric potentials such that $V_0 = 0$. It can be shown¹⁹ that the conductance in the d.c. limit is proportional to the trace of the product of current and the source vertices. It follows then that the line and the row, corresponding to I_0 and V_0 are identically zero, and we omit them for clarity below. The remaining four components are non-zero and we obtain the conductance matrix

in the general form

$$\begin{aligned} \hat{G} &= \begin{pmatrix} G_{aa} & G_{ab} \\ G_{ba} & G_{bb} \end{pmatrix} \\ &= \begin{bmatrix} \frac{1}{2} \left(1 - \frac{1}{2} Tr(\tilde{\lambda}_3 \lambda_3)\right), & -\frac{1}{2\sqrt{3}} Tr(\tilde{\lambda}_3 \lambda_8) \\ -\frac{1}{2\sqrt{3}} Tr(\tilde{\lambda}_8 \lambda_3), & \frac{2}{3} \left(1 - \frac{1}{2} Tr(\tilde{\lambda}_8 \lambda_8)\right) \end{bmatrix} \end{aligned} \quad (18)$$

1. Conductance of Y-junction

For the particular choice of S given in (14) above we have

$$\begin{aligned} \hat{G} &= \begin{pmatrix} |t_1^2| + \frac{1}{2}|t_2^2|, & 0 \\ 0, & 2|t_2^2| \end{pmatrix} \\ &= \begin{pmatrix} \frac{1}{2}[1 - \cos\theta \cos\psi], & 0 \\ 0, & \sin^2\theta \end{pmatrix} \end{aligned} \quad (19)$$

We see that the new third variable γ does not appear in any of the components of the conductance. In addition, we show below that γ does not take part in the renormalization process. Hence, in line with the above argument, the general symmetric case is completely determined by two independent parameters, which can be ultimately chosen as the two non-zero components of the conductance matrix, $G_{aa} \equiv G_a$, $G_{bb} \equiv G_b$, Eq. (19). We will present two coupled RG equations for the two conductances G_a, G_b in Sec. IV B below.

It follows from the parametrization (19) of the conductances that the physically accessible area in the two-dimensional space of conductances is not simply given by the unit square, but is defined by

$$0 \leq G_b \leq 1 - 4(G_a - \frac{1}{2})^2 \quad (20)$$

We will see below that the boundary of the physical regime in G_a, G_b -space defined by (20) plays a special role in that all fixed points of the problem are located on the boundary. We will use this fact to our advantage when we consider the simplified structure of the RG-flow along the boundary curve.

In the most general case, the matrix of conductances has four independent components, in accordance with the analysis of the number of relevant parameters characterizing the general S -matrix given in²⁶.

It is worth to note the following property of the boundary (20). It was proven in²⁷ that the boundary of the region of allowed conductances, defined by Eq. (15), corresponds to the matrices S which can be made entirely real by certain ‘‘rephasing’’, i.e. multiplication of rows and columns of S by phase factors. It was also proven that one can recover S from G up to this ‘‘rephasing’’.²⁷ In our particular case (14) the ‘‘rephasing’’, leading to the real-valued last line and last column, is achieved by $diag[ie^{-i\gamma}, ie^{-i\gamma}, 1] \cdot S \cdot diag[i, i, e^{i\gamma}]$. It is then clear, that the boundary corresponds either to $\psi = 0, \pi$, or $\theta = 0, \pi$, which is indeed the case, as shown below (see also²⁶).

2. Conductance in the simple tunneling case

Let us now consider the special case when the S-matrix is characterized by only a single parameter, $\theta = \theta_4 = \theta_6$. This corresponds to the simplest model of tunneling from the tip into the wire. Then we have

$$\begin{aligned}\tilde{\lambda}_3 &= \cos\theta\lambda_3 - \frac{1}{\sqrt{2}}\sin\theta(\lambda_4 - \lambda_6) \\ \tilde{\lambda}_8 &= -\frac{\sqrt{3}}{2}\sin^2\theta\lambda_1 - \sqrt{\frac{3}{8}}\sin 2\theta(\lambda_4 + \lambda_6) \\ &\quad + \frac{1 + 3\cos 2\theta}{4}\lambda_8\end{aligned}\quad (21)$$

and the reduced conductance tensor follows as

$$\hat{G} = \begin{pmatrix} \sin^2 \frac{\theta}{2} & 0 \\ 0, & \sin^2 \theta \end{pmatrix}\quad (22)$$

We note that the conductances satisfy the relation $G_b = 1 - 4(G_a - \frac{1}{2})^2$, implying that the simple tunneling case traces the boundary of the physically allowed region in G_a, G_b -space, see (20). As we will see below this case is more than a specialization to a very simple physical model. It actually already contains the information on the fixed point structure of the RG flow of the general model. Its advantage is that the fixed points and even the conductances may be calculated analytically. The stability of the fixed points cannot be decided in this restricted model, as runaway flow away from the boundary may occur (see Sec. IV B below).

3. Conductance in the fully symmetric case

For the fully symmetric case with $t_1 = t_2 = \frac{1}{3}(e^{3i\theta} - 1)$ we have from Eq. (19)

$$\hat{G} = \begin{pmatrix} \frac{2}{3}\sin^2 \frac{3\theta}{2} & 0 \\ 0, & \frac{8}{9}\sin^2 \frac{3\theta}{2} \end{pmatrix}\quad (23)$$

which shows that the maximum transparency of the fully symmetric junction is reached at $\theta = \pi/3$ and corresponds to $G_a = 2/3$, $G_b = 8/9$. These values are smaller than the maximum (unity) values of the individual conductances, which according to (20) are attained at the points $G_a = 1/2$, $G_b = 1$ and $G_a = 1$, $G_b = 0$ in the $G_a - G_b$ - plane.

IV. RG EQUATION: UNIVERSAL CONTRIBUTIONS

A. Simple tunneling case

1. Lowest order

The renormalization of the S-matrix due to interaction can be understood by considering the simplest diagrams

in perturbation theory. To illustrate our approach, we consider first the special case of the S-matrix, $(\tilde{\theta}, \tilde{\phi}, \tilde{\psi}) = (\theta, 0, 0)$ in Eq. (10). Our consideration follows closely our analysis of the simpler case of one impurity in a Luttinger liquid wire.¹⁹ In comparison with this previous case, we now have a few channels of interaction in the Hamiltonian (8). For the reader's convenience, we now outline the basics of our approach (see also Sec. V).

Consider the causal Green's function for fermions $\mathcal{G}_{ij}(x, t; y, t') = -i\langle T_t \psi_{j,in}(x, t) \psi_{j,out}^\dagger(-y, t') \rangle$. In the non-interacting system ($g_j = 0$) and given our model assumption of equal Fermi velocities in the wires, we have $\mathcal{G}_{ij}(x, t; y, t') = \mathcal{G}(t' - t, y - x) S_{ji}^{\dagger}$, according to (3). Here the scalar quantity \mathcal{G} describes the kinetic part of the Green's function in the scattering states representation. For the Wick-rotated (imaginary time) quantity \mathcal{G} we have

$$\mathcal{G}(i\omega; z) = -iv_F^{-1} \text{sign}(\omega) \Theta(\omega z) e^{-\omega z/v_F}.$$

The renormalization of the junction is obtained by considering the d.c. limit of $\mathcal{G}_{lm}(x < -L, y > L, \omega \rightarrow +0)$, and the contribution of interaction terms order-by-order. Without interaction we have in this limit $-iS_{lm}^*$, when we set $v_F = 1$. The renormalized S-matrix is then defined by $-iS_{lm}^*|_r = \lim_{\omega \rightarrow +0} \mathcal{G}_{lm}(\omega; x < -L, y > L)$. The first correction to $\mathcal{G}_{lm}(x, 0; y, t)$ in the basis of scattered states is of the form

$$\begin{aligned}\delta\mathcal{G}_{lm}(x, t; y, t') &= 2\pi g_k \int dz \int d\tau \langle \psi_l(x, 0) \\ &\quad \times (\psi_{i'}^\dagger(-z, \tau) \tilde{\rho}_k^{i'i''} \psi_{i''}(-z, \tau)) \\ &\quad \times (\psi_{j'}^\dagger(z, \tau) \tilde{\rho}_k^{j'j''} \psi_{j''}(z, \tau)) \psi_j^\dagger(y, t) \rangle S_{jm}^*,\end{aligned}$$

where summation over repeated indices is implied, and the matrices ρ_k and $\tilde{\rho}_k$ are given in (4). The two possible ways of contraction of the fermion operators lead to the expressions

$$2\pi g_k \mathcal{G}(\tau, -z - x) \rho_k^{lj'} \mathcal{G}(t' = 0, 2z) \tilde{\rho}_k^{j'j} \mathcal{G}(t - \tau, y - z) S_{jm}^*,$$

and

$$2\pi g_k \mathcal{G}(\tau, z - x) \tilde{\rho}_k^{li'} \mathcal{G}(t' = 0, -2z) \rho_k^{i'j} \mathcal{G}(t - \tau, y + z) S_{jm}^*.$$

Multiplying these expressions by $e^{i\omega t}$ and integrating over τ, t , we note that the dependence on x and y disappears in the limit $\omega \rightarrow 0$. The renormalized value of $-iS_{lm}^*$ is hence of the form

$$\begin{aligned}-iS_{lm}^*|_r &= -iS_{lm}^* - 2\pi g_k \int dz \left(\rho_k^{lj'} \mathcal{G}(t' = 0, 2z) \tilde{\rho}_k^{j'j} \right. \\ &\quad \left. + \tilde{\rho}_k^{li'} \mathcal{G}(t' = 0, -2z) \rho_k^{i'j} \right) S_{jm}^*,\end{aligned}$$

or, symbolically,

$$S_r^* . S = 1 - 2\pi i g_k \int dz \left(\mathcal{G}(0, 2z) \rho_k \tilde{\rho}_k + \mathcal{G}(0, -2z) \tilde{\rho}_k \rho_k \right).$$

The above correction may be interpreted as the self-energy Fock diagrams Σ_F , since the renormalized propagator may be represented generally in terms of the self-energy as Σ as $\mathcal{G}_r(-L, L) = \mathcal{G}_0(-L, L) + \mathcal{G}_0(-L, y)\Sigma(y, z)\mathcal{G}_0(z, L)$, where integration over y, z is implied. Using $G(0, 2z) = -i/4\pi z$, we may write this correction (first at $g_3 = 0$) as

$$\begin{aligned}\Sigma_F &= -g \int_{a_0}^L \frac{dz}{2z} ([\rho_+, \tilde{\rho}_+] + [\rho_-, \tilde{\rho}_-]) \\ &= -\frac{g}{4} \Lambda \frac{i(\lambda_4 + \lambda_6)}{\sqrt{2}} \sin \theta (1 + \cos \theta)\end{aligned}\quad (24)$$

with $\Lambda = \ln(L/a_0)$. We see that the matrix Green's function receives an off-diagonal static correction, signalling the necessity to redefine the rotation angle θ in the representation (10) of the S -matrix. It is remarkable that the above correction may be interpreted as a change of the angle θ , $\delta\theta$, as it is directed along the initial vector, i.e., along $\lambda_4 + \lambda_6$. This means that in the case of simple tunneling we are allowed to consider only a single renormalization equation for θ , as opposed to a set of three RG equations for θ , ψ and γ .

In the presence of the interaction in the third wire, contributing a term $g_3\rho_3\tilde{\rho}_3$ in the Hamiltonian, the changes in the above expression for Σ in first order of the interaction are minimal. In addition to the above combination $g([\rho_+, \tilde{\rho}_+] + [\rho_-, \tilde{\rho}_-])$ we should add $g_3[\rho_3, \tilde{\rho}_3]$, but since $[\rho_+, \tilde{\rho}_+] \sim [\rho_3, \tilde{\rho}_3] \sim [\lambda_8, \tilde{\lambda}_8]$ we obtain

$$\begin{aligned}\Sigma &= i(\lambda_4 + \lambda_6)\delta\theta/\sqrt{2}, \\ \delta\theta &= -\frac{1}{4}\Lambda (g \sin \theta + (g + 2g_3) \sin \theta \cos \theta)\end{aligned}\quad (25)$$

This equation (considering it as a precursor to the RG equation) is equivalent to Eq.(8) in²¹ (see also⁶).

In our previous work,¹⁹ we showed that the renormalization of the impurity in the Luttinger liquid can be analyzed within the fermionic formalism. The change of θ induced by the interaction and calculated in first order perturbation theory in (25) may now be used to obtain the renormalization group equation for θ in lowest order

$$\frac{d\theta}{d\Lambda} = -\frac{1}{4} (g \sin \theta + (g + 2g_3) \sin \theta \cos \theta) \quad (26)$$

In our earlier work we showed that higher order terms in the interaction may be summed in a systematic way, to access the strong coupling domain. In particular, we showed that the one-loop contributions to the RG equations for the S -matrix form a ladder series, which can be resummed by solving an integral equation of the Wiener-Hopf type. The result of this summation reproduces the known results obtained with the bosonization method for the weak and strong impurity case. It is found to be universal in the sense that it does not depend on the choice of regularization of the logarithmic divergences in the theory. We also showed that two-loop RG contributions are absent and the three-loop RG corrections are not universal but are not very sizeable in the whole range for a realistic choice of model parameters.

Let us now discuss how our method can be extended to the situation of the Y-junction. First we discuss the ladder summation, then we present the results of a computer symbolic calculation of the three-loop terms.

2. Ladder summation

Our previous solution of the ladder equation¹⁹ amounted to a the dressing of the interaction in the presence of the impurity. It thus led to a replacement $g \rightarrow \tilde{g}$ in an equation analogous to (26) with

$$\tilde{g} = \frac{2g}{1 + \sqrt{1 - g^2} - gY} \quad (27)$$

where $Y = Tr(\rho_- \tilde{\rho}_-)$; notice the different sign in front of gY here, which is a result of the different parametrization of the S -matrix in our previous work.

In view of the symmetry $1 \leftrightarrow 2$, we have $Tr(\lambda_3 \tilde{\lambda}_8) = Tr(\tilde{\lambda}_3 \lambda_8) = 0$. This means that the symmetric density combinations remain orthogonal after the scattering $Tr(\rho_- \rho_+) = Tr(\tilde{\rho}_- \tilde{\rho}_+) = Tr(\rho_- \tilde{\rho}_+) = Tr(\tilde{\rho}_- \rho_+) = 0$. This property allows us to perform the ladder summation separately in each of the channels, as described below.

First we consider the simpler case of $g_3 = 0$, the absence of interaction in the third wire. From Eq. (21) we have $Tr(\rho_- \tilde{\rho}_-) = \cos \theta$ and $Tr(\rho_+ \tilde{\rho}_+) = \frac{1}{4}(3 + \cos 2\theta)$. The ladder summation of the one-loop RG contributions in each channel is performed along the previous guidelines¹⁹ and the resulting RG equation is written as

$$\begin{aligned}\frac{d\theta}{d\Lambda} \equiv \beta(\theta) &= -\frac{g}{4} \sin \theta \left(\frac{2}{1 + d - g \cos \theta} \right. \\ &\quad \left. + \frac{2 \cos \theta}{1 + d - (g/4)(3 + \cos 2\theta)} \right)\end{aligned}\quad (28)$$

with $d = \sqrt{1 - g^2}$.

Let us now discuss the simultaneous presence of $g, g_3 \neq 0$. The result of the summation in the ρ_- channel is the same, whereas the channels ρ_+ and ρ_3 begin to mix in higher orders of the interaction. We omit the details of the derivation below and only provide intuitive arguments for the result obtained.

The dressing of the interaction occurs in the individual wires, characterized by two density components ρ_+, ρ_3 , which are orthogonal before the scattering, $Tr(\rho_+ \rho_3) = 0$. If these density components were orthogonal to those after the scattering, ($Tr(\rho_+ \tilde{\rho}_3) = Tr(\rho_+ \tilde{\rho}_+) = 0$, etc.) then the dressed interaction would simply be given by (27) with $Y = 0$. We define renormalized interaction constants in the form of two "charges" q, q_3 by $g \rightarrow 2g/(1 + \sqrt{1 - g^2}) = 2q^{-1}$, $g_3 \rightarrow 2g_3/(1 + \sqrt{1 - g_3^2}) = 2q_3^{-1}$ and introduce the diagonal matrix $\hat{Q} = diag[q, q_3]$ here.

According to Eq. (4) the two density components ρ_+, ρ_3 are connected to a vector of scattering eigenmodes,

$\phi = (\lambda_0, \lambda_8)/\sqrt{2}$, by

$$\begin{aligned} \begin{pmatrix} \rho_+ \\ \rho_3 \end{pmatrix} &= \frac{1}{\sqrt{2}} \hat{U} \begin{pmatrix} \lambda_0 \\ \lambda_8 \end{pmatrix}, \\ \hat{U} &= \frac{1}{\sqrt{3}} \begin{pmatrix} \sqrt{2} & 1 \\ 1 & -\sqrt{2} \end{pmatrix}, \end{aligned} \quad (29)$$

with $\hat{U}^2 = 1$ and $\text{Tr}(\phi_i \phi_j) = \delta_{ij}$. Notice that the modes λ_0 and λ_8 remain orthogonal both before and after the scattering, which is reflected in the matrix $\hat{Y} = \text{Tr}(\phi_i \hat{\phi}_j) = \text{diag}[1, \frac{1}{4}(1 + 3 \cos 2\theta)]$. The result of the ladder summation is represented by the matrix $(\hat{Q} - \hat{U} \hat{Y} \hat{U})^{-1}$.

The renormalization of the S -matrix in the first order occurs due to the non-vanishing commutators of densities $[\rho_+, \tilde{\rho}_+]$, $[\rho_3, \tilde{\rho}_3]$. Going to higher orders in the interaction, we have to take into account also the mixed commutators, $[\rho_+, \tilde{\rho}_3]$, $[\rho_3, \tilde{\rho}_+]$. Noticing that the only non-commuting components here are λ_8 and $\tilde{\lambda}_8$, and using Eq. (29), we find that the effect of renormalizing the interaction amounts to the replacement

$$(g + 2g_3) \sin 2\theta \rightarrow 6 \left[\hat{U} \hat{Q} \hat{U} - \hat{Y} \right]_{22}^{-1} \sin 2\theta, \quad (30)$$

which leads to the explicit result for the β -function in the ladder approximation:

$$\begin{aligned} \beta_L(\theta) &= -\frac{1}{2} \left(\frac{2 \sin 2\theta}{Q - \cos 2\theta} + \frac{\sin \theta}{q - \cos \theta} \right), \\ Q &= \frac{4qg_3 - 2q - 3q_3 + 1}{2q + q_3 - 3}, \\ q &= \frac{1 + K}{1 - K}, \quad q_3 = \frac{1 + K_3}{1 - K_3}, \\ K &= \sqrt{\frac{1 - g}{1 + g}}, \quad K_3 = \sqrt{\frac{1 - g_3}{1 + g_3}}, \end{aligned} \quad (31)$$

where we also provide the alternative definition of q, q_3 through the Luttinger parameters K, K_3 .

The equation (31) is a central result of this paper, and we analyze it in some detail in the next subsection. It should be noted that in the limit $g_3 \rightarrow 0$ and for small g this equation reduces to the Eq. (1) of Ref. [22], where the fixed points of the point contact model were discussed. We confirm Eq. (31) by calculating the perturbative corrections to the S -matrix up to the third order of the interaction in Sec. V.

3. Explicit solution of the RG equation

Let us analyze the RG equation (31). Introducing the variable $x = \cos \theta$, which determines the conductivity components via (22), we rewrite it in the form

$$\begin{aligned} \frac{dx}{d\Lambda} &= \frac{1}{2}(1 - x^2) \left(\frac{4x}{Q + 1 - 2x^2} + \frac{1}{q - x} \right), \\ &= \frac{3}{2}(x^2 - 1) \frac{(x - x_3)(x - x_4)}{(x^2 - q_0)(x - q)}, \end{aligned} \quad (32)$$

with

$$\begin{aligned} q_0 &= \frac{1}{2}(Q + 1), \\ x_{3,4} &= \frac{1}{3}[q \mp \sqrt{3q_0 + q^2}], \end{aligned} \quad (33)$$

Here Q is defined in (31). The zeros of the r.h.s., the four fixed points (FPs) of the RG equation, are given by $x_{1,2} = \pm 1$, and $x_{3,4}$. For later reference we label the fixed points x_1, x_2, x_3, x_4 as N, A, M, Q . Fixed point N corresponds to $G_a = G_b = 0$, i.e. the three wires are separated. At fixed point A we have $G_a = 1, G_b = 0$, i.e. the third wire is disconnected whereas the main wire is perfectly conducting. The fixed points M, Q are located on the boundary of the physically accessible region, unless they are outside the region defined by (20).

For repulsive interaction, $0 < K, K_3 < 1$, the fixed point $x_4 > 1$ is outside the physical domain, $|x| \leq 1$. One can easily verify that the two fixed points N, A at $x_{1,2} = \pm 1$ are stable, i.e. $d\beta/dx|_{x_{1,2}} < 0$. We will see below that A turns unstable in the general symmetric case. Fixed point M at $x_3 \in (-1, 0)$ is unstable. At weak coupling, we write $K = 1 - g$ and $K_3 = 1 - g_3$ with $0 < g^2 \ll g, g_3 \ll 1$, and get $x_3 \simeq -g/(g + 2g_3)$, cf.²²

The equation (32) may be integrated to give the implicit solution for x as a function of the length L in the form

$$\begin{aligned} F[x(L)] &= (1 - x)^{\gamma_1} (1 + x)^{\gamma_2} |x - x_3|^{\gamma_3} |x - x_4|^{\gamma_4} \\ &= F[x(L_0)] L/L_0, \end{aligned} \quad (34)$$

where

$$\begin{aligned} \gamma_1 &= \frac{1}{3} \frac{(1 - q_0)(1 - q)}{(1 - x_3)(1 - x_4)} \\ &= - (K^{-1} + K_3^{-1} - 2)^{-1}, \\ \gamma_2 &= \frac{1}{3} \frac{(1 - q_0)(1 + q)}{(1 + x_3)(1 + x_4)} \\ &= - \left(\frac{1}{2}(K^{-1} + K - 2) + K_3^{-1} - 1 \right)^{-1}, \\ \gamma_3 &= \frac{2}{3} \frac{q - x_3}{x_4 - x_3} \frac{q_0 - x_3^2}{1 - x_3^2}, \\ \gamma_4 &= -\frac{2}{3} \frac{q - x_4}{x_4 - x_3} \frac{q_0 - x_4^2}{1 - x_4^2}, \end{aligned} \quad (35)$$

We see that the fixed point N at $x = 1$, corresponding to three fully detached wires, is characterized by the exponent γ_1 , which is determined by the sum of two boundary exponents, K^{-1} and K_3^{-1} . The second fixed point A at $x = -1$, corresponding to the ideal wire 1 and 2 and

the detached wire 3, relates to the exponent γ_2 , which is governed by the boundary exponent of the third wire, K_3^{-1} , and the bulk anomalous dimension of the fermion operator $(K^{-1} + K)/2$, the latter quantity defining the local density of states in tunneling experiments.

In the important special case of arbitrary but equal interaction strength, $K_3 = K$ we have $Q = (4q - 1)/3$, $q_0 = (2q + 1)/3 = x_4$ and $x_3 = -1/3$. The expressions for $\gamma_{3,4}$ simplify and we have

$$\begin{aligned}\gamma_3^{-1} &= 6 \frac{1 - K}{(2 + K)^2}, \\ &= \frac{2}{3}(K^{-1} - 1) - \frac{2}{3} \frac{4 - K}{(2 + K)^2} (K^{-1} + K - 2), \quad (36) \\ \gamma_4^{-1} &= -6 \frac{3 - K}{K(3 + K)},\end{aligned}$$

For completeness, we also consider the case of attractive interaction $K, K_3 > 1$. First of all, the role of the fixed points is reversed, so that the fixed points N, A at $x = \pm 1$ are unstable and the third fixed point M at x_3 becomes stable. Further, we observe that while for repulsive interaction $x_4 > 1$ always lies outside the physical region of x , this is different in the attractive case. For simplicity, let us first consider the case of equal interaction in the wires, $K = K_3$. We have $x_3 = -1/3$ and the value of $x_4 = (2q + 1)/3 = \frac{3+K}{3(1-K)}$ reaches the physical range of x first and coincides with $x = -1$ at $K = 3$. At this point the inverse exponents $\gamma_2^{-1} = \gamma_4^{-1} = 0$. A subsequent increase of K takes $-1 < x_4 < -1/3$ inside the physical domain. One can verify that the fixed point Q at x_4 in this latter case is unstable, whereas the fixed point A at the edge $x = -1$ becomes stable.

Another interesting possibility for attractive interaction is merging of the points x_3 and x_4 . It happens at $3q_0 = -q^2$ in (33), or at

$$K_3 = 2K \frac{1 + K^3}{(1 + K)^2(2K - 1)},$$

and the position of FP in this case is

$$x_3 = x_4 = \frac{1}{3}(1 + K)/(1 - K).$$

The last equations show, that in order to have $|x_{3,4}| < 1$ one should let $K \geq 2$, $K_3 \geq 4/3$. We return to these questions below in Sec. VI, when discussing the ‘‘phase diagram’’ of our model.

B. General Y junction

Let us now analyze the general case of the S -matrix, Eq. 10. As shown above in Sec. IV A 1, the RG flow to first-order in the interaction is determined by two contributions, which are proportional to $[\tilde{\lambda}_3, \lambda_3]$ and $[\tilde{\lambda}_8, \lambda_8]$. We write

$$S^{-1} \cdot S_r - 1 = \Lambda(\alpha_3[\tilde{\lambda}_3, \lambda_3] + \alpha_8[\tilde{\lambda}_8, \lambda_8]), \quad (37)$$

where $\alpha_3 = -g/4, \alpha_8 = -(g + 2g_3)/12$ are introduced for brevity. Comparing the right-hand side of the above expression with the parametrization (12) of the S -matrix, we can find the corresponding change of the parameters $\tilde{\theta}, \phi, \tilde{\psi}$ in the renormalized scattering matrix S_r .

After some calculation we find the following set of RG equations

$$\begin{aligned}\frac{d\tilde{\theta}}{d\Lambda} &= \alpha_3(\cos \tilde{\psi} \sin \tilde{\theta} + \sin \tilde{\psi} \cos \tilde{\theta} \sin \phi) \\ &\quad + 3\alpha_8 \cos \tilde{\theta} \sin \tilde{\theta} \cos^2 \phi, \\ \frac{d\phi}{d\Lambda} &= \alpha_3 \frac{\cos \phi \sin \tilde{\psi}}{\sin \tilde{\theta}} - 3\alpha_8 \sin \phi \cos \phi, \\ \frac{d\tilde{\psi}}{d\Lambda} &= 3\alpha_3(\cos \tilde{\psi} \sin \tilde{\theta} \sin \phi + \sin \tilde{\psi} \cos \tilde{\theta}).\end{aligned} \quad (38)$$

At first sight, there are three equations for three parameters. However, one can check that $d\tilde{\psi}/d\Lambda = 3\cos^2 \tilde{\theta} d(\sin \phi \tan \tilde{\theta})/d\Lambda$, irrespective of the interaction, so that only two of the equations are independent.

Indeed, using the equivalent parametrization of the S -matrix in the form Eq. (14), we obtain the RG equations in the new variables θ, ψ, γ as :

$$\begin{aligned}\frac{d\theta}{d\Lambda} &= \sin \theta(\alpha_3 \cos \psi + 3\alpha_8 \cos \theta), \\ \frac{d\psi}{d\Lambda} &= \alpha_3 \sin \psi \left(3 \cos \theta + \frac{1}{\cos \theta} \right), \\ \frac{d\gamma}{d\Lambda} &= \alpha_3 \frac{\sin \psi}{\cos \theta}\end{aligned} \quad (39)$$

Therefore, we have only two independent RG equations (39) for the variables θ and ψ , which define the components of the conductance matrix (19). The third component γ is not independent and is determined by θ and ψ ; it does not enter the conductance.

It is also instructive to express the RG equations directly in terms of the components of the conductance tensor (18). We introduce

$$\begin{aligned}a &= \frac{1}{2} \text{Tr}(\tilde{\lambda}_3 \lambda_3) = \cos \theta \cos \psi, \\ b &= \frac{1}{2} \text{Tr}(\tilde{\lambda}_8 \lambda_8) = \frac{1}{4}(1 + 3 \cos 2\theta),\end{aligned} \quad (40)$$

so that the conductance matrix is $\hat{G} = \text{diag}(\frac{1}{2}(1 - a), \frac{2}{3}(1 - b))$. From (39) we find

$$\begin{aligned}\frac{da}{d\Lambda} &= -2\alpha_3(1 + b - 2a^2) - 2\alpha_8(1 - b)a, \\ \frac{db}{d\Lambda} &= -2(1 - b)(\alpha_3 a + \alpha_8(1 + 2b)),\end{aligned} \quad (41)$$

or, directly in terms of conductance,

$$\begin{aligned}\frac{dG_a}{d\Lambda} &= \alpha_3(8G_a(1 - G_a) - \frac{3}{2}G_b) + \frac{3}{2}\alpha_8 G_b(1 - 2G_a), \\ \frac{dG_b}{d\Lambda} &= 2\alpha_3 G_b(1 - 2G_a) + 6\alpha_8 G_b(1 - G_b),\end{aligned} \quad (42)$$

Comparing Eq. (39) to the above special case, ($\psi = \gamma = 0$), we observe that the arguments, leading to the possibility of the ladder summation in Sec. IV A 2, remain valid. Hence we can use the previous result, which amounts to the substitution

$$\begin{aligned}\alpha_3 &= -\frac{1}{2} \frac{1}{q-a} = -\frac{1}{2} \frac{1}{q-1+2G_a}, \\ \alpha_8 &= -\frac{1}{2} \frac{1}{Q_1-b} = -\frac{1}{2} \frac{1}{Q_1-1+\frac{3}{2}G_b}, \\ Q_1 &= \frac{3qq_3 - q - 2q_3}{2q + q_3 - 3}\end{aligned}\quad (43)$$

with q, q_3 defined in (31). The equations (41), (42), (43) are the main result of this paper.

Notice that the RG equation for the quantity

$$\begin{aligned}G_{\perp} &= G_b + (2G_a - 1)^2, \\ &= \frac{2}{3}(1-b) + a^2 = 1 - \cos^2 \theta \sin^2 \psi,\end{aligned}\quad (44)$$

due to Eq. (42) has a form

$$\frac{dG_{\perp}}{d\Lambda} \propto (1 - G_{\perp}) \quad (45)$$

which, together with (20) and second line in (42), shows that the boundaries for the observable conductances for free fermions, $G_{\perp} = 1$ and $G_b = 0$, are the RG fixed lines in the interacting case.

Concerning the character of the fixed points in this more general situation, there is a qualitative change. In the tunneling case, and for repulsive interaction, we had two stable FPs, A, N , corresponding to i) one wire detached ($x = -1$) and ii) three wires detached ($x = 1$). The unstable FP M (x_3) was located between these two limiting cases.

Now we have two independent components of the conductance. We find only one truly stable FP: N , the case of all three wires detached, $G_a = G_b = 0$. The previous stable FP A with one wire detached ($G_a = 1, G_b = 0$) transmutes into a saddle point, so it is not truly stable. The third (unstable) FP M is at the boundary of the region of conductances in the $G_a - G_b$ -plane allowed by unitarity and is unstable in both directions.

The RG flows for repulsive interactions of strength $g = 0.2, g_3 = 0.03$ are depicted in Fig. 2. It is interesting to note that the three representative flow trajectories emanating from fixed point M indicate nonmonotonic behavior of G_b (black) or of G_a (red) as a function of, e.g. temperature. As shown in²² this behavior at $g_3 = 0$ appears first in second order perturbation theory in the interaction g . It was demonstrated there, that the intermediate M point at $g_3 = 0$ appears due to the competition between the bulk zero-bias anomaly and the scattering off Friedel oscillations induced by the third wire. This underlines the difference in the origin of the intermediate point in Ref. [22] and the origin of the intermediate point in this and other studies^{6,7,16,18,21} with $g_3 \neq 0$.

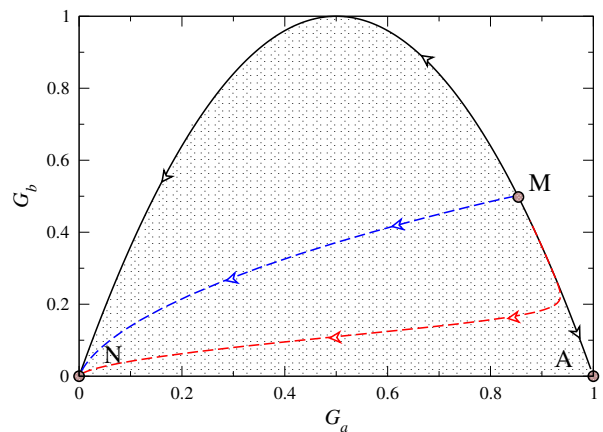


FIG. 2: (Color online) Ladder approximation for the β -function and RG flows for $g = 0.2$ and $g_3 = 0.03$. Three fixed points are shown by dots and are: (i) stable one at $G_a = G_b = 0$, (ii) unstable one at $G_a \simeq 0.8542, G_b \simeq 0.4979$, and (iii) saddle-point type fixed point at $G_a = 1, G_b = 0$. The values of conductances, allowed by unitarity, are shown as a shaded region.

The scaling behavior in the case of attractive interaction is even more interesting (although attractive effective interaction is not easily realized in nature!). The conductances at M are given by $G_a = (1 - x_3)/2$ and $G_b = 1 - x_3^2$, where x_3 is given in (33). As mentioned above, fixed point N becomes unstable, while M is stable. In the case of not too strong attractive interaction, $1 < K, K_3 < 3$, M is the only stable fixed point. Again the behavior of both, G_a and G_b may be nonmonotonic. For even stronger attractive interaction the fourth fixed point Q enters the physically accessible region as a further unstable FP. This leads to a switch of fixed point A from unstable to stable. In Fig. 3 the flow diagram is shown for strong attractive interaction, $K = K_3 = 3.7$.

It is useful to analyze the RG equations (41) around the N and A fixed points. For the N point which corresponds to $a = b = 1$ we write $a = 1 - a', b = 1 - b'$ and find in the leading order of the small deviations $a' > 0, b' > 0$:

$$\begin{aligned}\frac{d}{d\Lambda} (a' - \frac{1}{3}b') &\simeq 2(1 - K^{-1}) (a' - \frac{1}{3}b'), \\ \frac{d}{d\Lambda} b' &\simeq (2 - K^{-1} - K_3^{-1}) b'.\end{aligned}\quad (46)$$

Similarly, around the A with $a = -b = -1$ we expand $a = -1 + a', b = 1 - b'$ to obtain:

$$\begin{aligned}\frac{d}{d\Lambda} (a' - \frac{1}{3}b') &\simeq 2(1 - K) (a' - \frac{1}{3}b'), \\ \frac{d}{d\Lambda} b' &\simeq \left(1 - K_3^{-1} - \frac{(1 - K)^2}{2K}\right) b'.\end{aligned}\quad (47)$$

In the equations (46), (47) the combination $a' - \frac{1}{3}b' > 0$ measures the distance to the parabola $b = (3a^2 - 1)/2$ of the simple tunneling case $\psi = 0$ in (40). Thus we confirm that the border lines of the physical sector of

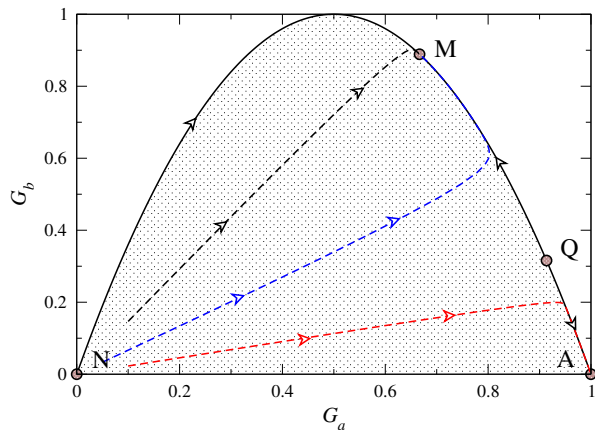


FIG. 3: (Color online) Ladder approximation for the β -function and RG flows for $K = K_3 = 3.7$. Four fixed points are shown by dots and are: (i) unstable one at $G_a = G_b = 0$, (ii) stable one at $G_a = 1, G_b = 0$, (iii) stable one at $G_a = 2/3, G_b = 8/9$ and (iv) new (appearing at $K > 3$) unstable fixed point at $G_a \simeq 0.9136, G_b \simeq 0.3159$. The values of conductances, allowed by unitarity, are shown as a shaded region.

conductances, Eq. (20), are the “fixed lines” of our RG equations.

The meaning of scaling exponents in (46), (47) is as follows. The quantity $a' - \frac{1}{3}b'$ is the difference of the Y-junction from the simple tunneling case which may arise primarily due to impurity scattering located in the main wire. It is then quite natural that it scales at N point with the usual double exponent, $2(1 - K^{-1})$, of the weak tunneling between two equal Luttinger liquids. The quantity b' stands for the tunneling conductance and its exponent combines the weak tunneling contributions from the main and the third wire. At the fixed point A we have the conductance $G_b = \frac{2}{3}b'$ defined by the weak tunneling from the third wire, $(1 - K_3^{-1})$, into a perfect Luttinger liquid with a bulk exponent $(1 - K)^2/2K$. The small value of $a' - \frac{1}{3}b'$ in this case corresponds to a weak barrier in the main wire, which scales with the exponent $2(1 - K)$.^{22,28}

C. Fully symmetric Y junction

In this section we consider the case of full symmetry between the wires, which means equal strength of interactions, $K = K_3$. The asymmetry at the Y-junction may still lead to an asymmetry in the physical properties of our system. However, it is a remarkable fact that the symmetric Y-junction, $a = b$, in other terms $G_b = \frac{4}{3}G_a$, remains a fixed line in this case.

We observe that for $K = K_3$ we have $q = q_3 = Q_1$ and $\alpha_3 = \frac{1}{2}(a - q)^{-1}$, $\alpha_8 = \frac{1}{2}(b - q)^{-1}$ in (43). Introducing the symmetrized variables, $c = b - a$, $\bar{a} = (a + b)/2$, we

obtain from Eq. (41)

$$\begin{aligned} \frac{d\bar{a}}{d\Lambda} &= \frac{(1 - \bar{a})(1 + 3\bar{a})}{q - \bar{a}} + \mathcal{O}(c^2), \\ \frac{dc}{d\Lambda} &= \frac{1 + 3\bar{a}^2 - 4\bar{a}q}{(q - \bar{a})^2}c + \mathcal{O}(c^2). \end{aligned} \quad (48)$$

This set of equations shows that the RG flows form a “spindle” shape around the line $a = b$, with two edge FPs at $a = b = 1$ (N point) and $a = b = -1/3$ (M point). The first equation in (48) is easily integrated with the result (cf. (34))

$$\tilde{F}[\bar{a}(L)] = (1 - \bar{a})^{\gamma_2} \left(\frac{1}{3} + \bar{a}\right)^{\gamma'_3} = \tilde{F}[\bar{a}(L_0)] L/L_0 \quad (49)$$

here $\gamma_2^{-1} = -2(K^{-1} - 1)$ follows from (35) and

$$(\gamma'_3)^{-1} = 6 \frac{1 - K}{(2 + K)}. \quad (50)$$

Notice that the similar-looking γ_3 in (36) defines the scaling exponent for c in (48).

V. PERTURBATION THEORY AND NON-UNIVERSAL TERMS

The ladder summation discussed above captures contributions of a certain type (one-loop) to all orders in the interaction. By its structure it is similar to the RPA summation scheme, which works perfectly well for the description of the bulk properties of a Luttinger liquid, due to the absence of multi-tail fermionic loops in the linearized dispersion model²⁹. There remains the question of the importance of higher loop contributions. In our work on the Luttinger liquid with barrier we were able to show in perturbation theory that the two-loop contribution vanishes and the three-loop contribution is subdominant in the neighborhood of the fixed points. As a result, the exponents of the power laws of the conductance in length L or temperature T turned out to be in exact agreement with those obtained by methods of bosonization, and the thermodynamic Bethe ansatz. In this section we explore to which extent a similar result is true in the case of a Y-junction.

A. Simple tunneling case

The symbolic computation of the diagrams up to the third order can be performed as explained in the previous work.¹⁹ The diagrammatic rules are similar, with the only difference that we have 3×3 matrices for the vertices now. This means that the kinematic structure for each diagram is the same both for the Y-junction and for the barrier in the Luttinger liquid. Therefore we can use the previously obtained results for the individual diagrams, while supplying them with different matrix prefactors.

We may represent the renormalized scattering matrix, S_r , in the form

$$S^\dagger \cdot S_r = 1 + g\Sigma_1 + g^2\Sigma_2 + g^3\Sigma_3 + \dots, \quad (51)$$

(in the presence of both g and g_3 we consider Σ_j as dependent on the ratio g_3/g). In the next step, we verify the functional form of the matrix $S^\dagger \cdot S_r = \exp i\delta\theta(\lambda_4 + \lambda_6)/\sqrt{2}$ and determine the scalar quantity $\delta\theta$ as a function of $g, \theta, \Lambda, g_3/g$. We have for the renormalized value $\theta_r = \theta + \delta\theta(\theta) = f(\theta, g\Lambda, g)$ and inverting this equality we may write $\theta = f^*(\theta_r, g\Lambda, g)$. Demanding now that the initial "bare" value θ should not depend on Λ , we may derive the RG equation.¹⁹

Following these steps, we arrive at an expression for the β -function, which we keep up to third order in g, g_3 . We compare this perturbative result with the Taylor expansion of Eq. (31) and confirm the identity of the two expressions up to second order in the interaction. In the third order of g , the direct calculation of the β -function provides the ladder contribution given by the corresponding term in the Taylor expansion of Eq. (31) and in addition a three-loop contribution to $\beta(\theta)$ beyond the ladder result. In accordance with Ref. [19], we find that this three-loop correction is a subleading contribution, stemming from the non-universal parts of the diagrams. As was explained in the previous work, performing the evaluation of the diagrams we find a few generic integrals, which contain non-universal numbers b_2, b_3, b_4 which for $T = 0$ are equal to $\pi^2/6, 2\ln 2, 2(\ln 2 - 1)$, respectively.³¹ The extra term in the β -function, which should be added to (31) is given by

$$\begin{aligned} \beta_3(\theta) &= \frac{g^3}{128} \sin^3 \theta (b_2 f_2 + b_3 f_3 + b_4 f_4) \\ f_2 &= 1 + 8z + 2z^2 + 4z^3 + (1 + 2g_3/g)^2 \\ f_3 &= (1 - z)^2 - 4g_3/g \\ f_4 &= 2(1 + z)(1 + z^2) \\ z(\cos \theta) &= (1 + 2g_3/g) \cos \theta \end{aligned} \quad (52)$$

Comparing with the case of the single wire with barrier we see that the f_j are now smooth functions of θ , rather than constants.

Let us consider the influence of $\beta_3(\theta)$ on the fixed point values defined by $\beta_L = 0$ of the reduced RG equation (31), as analyzed in the previous subsection. Near the two fixed points N, A , at $\theta = 0, \pi$, corresponding to $x = \pm 1$, the term (52) is small, proportional to the third power of $\sin \theta$. This means that neither the positions of these two fixed points, nor their scaling exponents $\gamma_{1,2}$ in (35) are affected by $\beta_3(\theta)$.

The position of the third fixed point, x_3 , is defined in the ladder approximation by $(g + 2g_3)x_3 + g = 0$, up to higher order corrections. The latter condition reads $z(x_3) = -1$ in (52), and we find accordingly that the f_j at x_3 are given by $f_2 = -4(2 + g_3/g)(1 - g_3/g)$, $f_3 = 4(1 - g_3/g)$, $f_4 = 0$. It follows that the position of the

third fixed point x_3 is affected by the β_3 term at $g_3 \neq g$; and the critical exponent γ_3 is affected in this case, too.

B. General Y-junction

We start as described above in Sec. V, but have to slightly modify our approach afterwards. It turns out that in the case of a general Y-junction the intermediate expressions produced in computer calculation show enormous complexity in the third order. The formulation in terms of the S -matrix followed in the above analysis becomes impractical.

However, we may find the logarithmic corrections to the conductance directly, in the spirit of our treatment of the impurity in the Luttinger liquid.¹⁹ Indeed, ultimately we need to analyze only the partial contributions to the two conductances, Eq. (40), rather than the full corrections to the S -matrix, i.e. 3×3 matrix quantities. Thus we may keep only these two partial contributions from each diagram, which drastically simplifies the calculation.

Another simplification occurring in the present analysis of the d.c. limit is the absence of vertex corrections in the diagrams for the conductances.¹⁹ As a result, it suffices to consider only the self-energy parts of the Green's functions, corresponding to the above Eq. (51). The absence of vertex corrections is easily proven in case of $T = 0$ which we consider in this paper. The analysis at $T \neq 0$ which was undertaken for the impurity in the Luttinger liquid,¹⁹ is more involved in case of the Y-junction and shall be given elsewhere.

Below we explain a few points of this analysis in more detail. Each diagram contributing, e.g., to the component $G_a = (1 - a)/2$ in (40), stems from the generic expression $a = \frac{1}{2}Tr(\lambda_3 G_{\omega=+0}^R \lambda_3 G_{\omega=+0}^A)$. Here we introduced the retarded (advanced) Green's functions $G^{R(A)} = \mp i\vartheta(\pm t)\langle[\psi(x, t), \psi^\dagger(y, 0)]\rangle$ with $x \rightarrow -\infty$, $y \rightarrow \infty$. When Fourier-transformed and taken at zero energy, the Green's functions are stripped from the coordinate dependence and become simply proportional to the S -matrix, $G^R = -iS^\dagger$, $G^A = iS$, (we set $v_F = 1$). The expansion (51) leads to the renormalized quantity

$$a_r = a_0 + ga_1 + g^2a_2 + g^3a_3 + \dots \quad (53)$$

where $a_0 = \frac{1}{2}Tr(\tilde{\lambda}_3\lambda_3)$ and

$$\begin{aligned} a_1 &= \frac{1}{2}Tr \left[\tilde{\lambda}_3(\Sigma_1\lambda_3 + \lambda_3\Sigma_1^\dagger) \right], \\ a_2 &= \frac{1}{2}Tr \left[\tilde{\lambda}_3(\Sigma_2\lambda_3 + \Sigma_1\lambda_3\Sigma_1^\dagger + \lambda_3\Sigma_2^\dagger) \right], \\ a_3 &= \frac{1}{2}Tr \left[\tilde{\lambda}_3(\Sigma_3\lambda_3 + \Sigma_2\lambda_3\Sigma_1^\dagger + \Sigma_1\lambda_3\Sigma_2^\dagger + \lambda_3\Sigma_3^\dagger) \right], \end{aligned} \quad (54)$$

and similarly for b_r , where the components Σ_j of the self energy have been defined in (51). The advantage of directly calculating corrections to a_r, b_r is most apparent

when dealing with the long expressions for Σ_3 . The partial contribution to a_3 has the form

$$\begin{aligned} \frac{1}{2}Tr \left[\tilde{\lambda}_3(\Sigma_3\lambda_3 + \lambda_3\Sigma_3^\dagger) \right] &= \frac{1}{2}Tr \left[\tilde{\lambda}_3\Sigma_3\lambda_3 \right] + h.c. \\ &= Re(Tr(\lambda_3\tilde{\lambda}_3\Sigma_3)). \end{aligned}$$

The expressions a_r, b_r obtained in this way show both, scale-dependent terms in the form of the logarithm of $\Lambda = L/a$ and in addition scale-independent terms, as is explained at length elsewhere.¹⁹ The result of this calculation provides expressions for the renormalized values of conductance, a_r, b_r , in terms of the bare ones, a, b . In the next step of the Callan-Symanzik scheme we are considering here, we invert these expansions, and express the bare values via the renormalized ones, keeping terms up to g^3 in the corresponding series.

Then we require that the bare values be independent of the scale in consideration, i.e. the logarithm Λ ,

$$\frac{da}{d\Lambda} = \frac{\partial a}{\partial \Lambda} + \frac{\partial a}{\partial a_r} \frac{\partial a_r}{\partial \Lambda} + \frac{\partial a}{\partial b_r} \frac{\partial b_r}{\partial \Lambda} = 0 \quad (55)$$

and similarly for $db/d\Lambda$. Solving this system of linear equations for the quantities $da_r/d\Lambda, db_r/d\Lambda$, we find:

$$\frac{d}{d\Lambda} \begin{pmatrix} a_r \\ b_r \end{pmatrix} = - \left(\frac{\partial a}{\partial a_r}, \frac{\partial a}{\partial b_r} \right)^{-1} \frac{d}{d\Lambda} \begin{pmatrix} a \\ b \end{pmatrix} \quad (56)$$

This calculation is best done by means of computer algebra, since the intermediate expressions are quite complicated.

We keep the terms of the order of g^3 in the final expressions. A criterion for the correctness of the calculation is the absence of any Λ -dependence on the right-hand side of Eq. (56) up to this order.

When we compare the final expressions, found in this direct calculation, with the first terms of the Taylor expansion of the corresponding expressions (41), (43), we find complete agreement of the universal (regularization independent) parts of the β -functions to third order. In addition to these universal contributions of the ‘‘one-loop’’ ladder summation (43), we also find non-ladder contributions β_3 , which first appear in third order and explicitly contain the above mentioned regularization-dependent coefficients b_j . These contributions are rather complicated and are listed in Appendix.

Comparing these three-loop contributions with the simpler case of one impurity in the Luttinger liquid, we should make several remarks. First of all, one can explicitly check that these contributions satisfy Eq. (45) so that the curve $G_\perp = 1$ remains the fixed line. Second, for small g, g_3 these terms do not lead to the appearance of extra FPs, but the situation with strong interaction $|g|, |g_3| \sim 1$ is, strictly speaking, unclear. However, we make a plausible conjecture, that all FPs of full RG beta function (which contains three loop, four loop etc. contributions, beyond the re-summed one-loop terms (42),

(43)) lie on the borderline of allowed conductances for the non-interacting case.

The next remark concerns the universality of the phase diagram, proposed below in Sec.VI on the basis of the expression (42), (43). What is the evidence that no new FPs appear at strong interaction, and the structure of the phase diagram is independent of regularization? The answer to this question goes along several lines. From the actual form of three-loop contributions we see that regularization does not change the position of the interaction-dependent FP M only in fully symmetric case. However, in the latter case the three loop terms are apparently unimportant even in the strongly interacting regime, as is suggested by comparison of our results with those in¹⁸. The bosonization approach by Oshikawa et al. showed changes in the character of A fixed point at strong attraction, $K = K_3 = 3$, and we see the appearance of FP Q at this value. The scaling dimensions of leading perturbations, found in Sec. 10.1 and 10.4.2 of¹⁸, agree with our one loop formulas (46), (47) for the whole range of interaction strength.

In summary, we again find that the non-universal terms in the β -functions do not influence the behavior at the fixed points N, A , which means that the ladder summation is sufficient in the case of repulsive interactions. As for the fixed point M , of importance for attractive interaction, we find that the non-universal terms are relevant and may change the power law exponents in principle. We address this question in some detail in the next subsection.

C. Fully symmetric Y junction

In the important case of equal interactions, $g_3 = g$, the position of the third fixed point (M) in Eq. (32) is $\cos \theta = x_3 = -1/3$ and remains unaffected by β_3 in (52). Expanding β_3 around x_3 we have

$$\beta_3 = \frac{\sqrt{2}}{18} g^3 (x + 1/3)(4b_2 - b_3 + b_4) + \dots, \quad (57)$$

so that the scaling exponent along the limiting parabola, γ_3 in Eq. (36), depends on the non-universal coefficients b_j , which were found to depend on the regularization of the theory. The situation is however more delicate, because the scaling exponent γ_3' in (50) in the direction perpendicular to parabola remains unchanged by the three loop contributions. To see that we expand the expressions for β_3 listed in Appendix B. In terms of variables \bar{a}, c we have the additional three loop contributions to Eq. (48)

$$\begin{aligned} \frac{d\bar{a}}{d\Lambda} &= -g^3 \frac{2b_2 + b_4}{16} (1 - \bar{a})^2 (1 + 3\bar{a})^2 + \mathcal{O}(g^3 c^2), \\ \frac{dc}{d\Lambda} &= g^3 c \frac{\bar{a}(1 - \bar{a})}{8} (2b_2(5 + 7\bar{a}) + b_3(\bar{a} - 1) \\ &\quad + 4b_4(1 + 2\bar{a})) + \mathcal{O}(g^3 c^2). \end{aligned} \quad (58)$$

The second equation here at the M fixed point $\bar{a} = -1/3$ corresponds to (57). The first equation (58) together with (48) show that near the fixed points the three loop contributions do not change the scaling exponent γ'_3 of Eq. (50).

VI. DISCUSSION AND CONCLUSIONS

In this paper we presented a theory of charge transport through a junction of three quantum wires, modelled by Luttinger liquids. We focused on the case of a Y-junction, a set-up symmetric with respect to interchanging wires 1 and 2. We allow for different interaction strengths g and g_3 in wires 1, 2 and wire 3, respectively. Our method employs a purely fermionic representation, which has the advantage that the connection to ideal (noninteracting) leads is naturally incorporated. The transition from the noninteracting leads to the interacting wire is assumed to be adiabatic. We find that at zero temperature the scattering process is completely described by elastic scattering (no excitation of real particle-hole pairs). Virtual excitations of multi particle-hole pairs are all-important; these processes are described in terms of the renormalized single particle S-matrix. In terms of diagrams for the conductances this amounts to the absence of any vertex corrections (at $T = 0$).

We extended a theory previously applied to a two-wire junction to the Y-junction problem. That theory employs perturbation theory with respect to the interaction in fermionic language (using, however, the concepts of current algebra to systematize the bookkeeping) to derive the renormalization group β -function for the conductance. As shown by us in Ref.¹⁹ an RPA type ladder summation of an infinite class of terms of perturbation theory may be performed to generate all of the known results on the scaling behavior of the conductance, power law exponents, crossover behavior, and more, for any interaction strength and any scattering characteristic of the barrier.

In the general time-invariant case the tensor of conductances features two independent components G_a, G_b . These components are confined to an area bounded by a curve B in the fundamental domain $0 < G_a, G_b < 1$. We derive the coupled set of RG-equations for conductances in the ladder approximation. It is interesting to note that the fixed points of these equations are all located on the boundary curve B . In fact a simplified tunneling model leads to conductances located on the boundary curve B , and allows for an analytical determination of the fixed points and the conductances.

We probe the validity of the ladder summation by evaluating all contributions up to and including third order (several thousands diagrams). We classify the contributions into universal (ladder summation) and non-universal, with respect to the regularization (finite length L or finite temperature T). For repulsive interaction we find that the non-universal contributions to the RG- β -

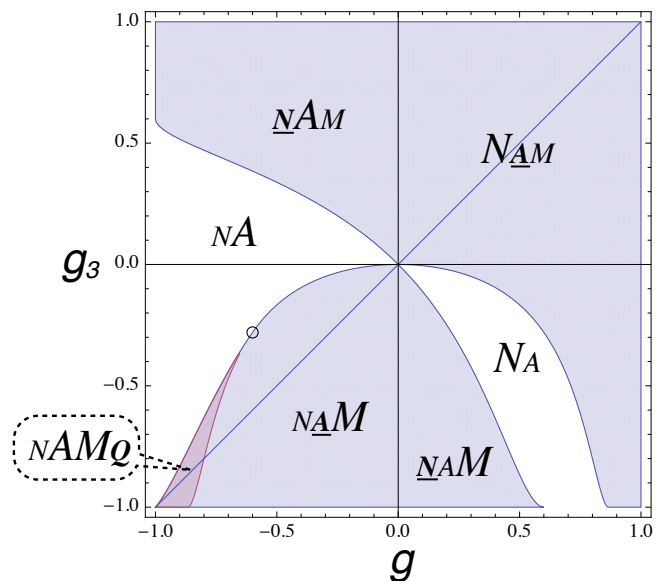


FIG. 4: (Color online) The number and the type of physically available fixed points is shown for various strength of interactions g and g_3 , as defined by the ladder summation. The positions of N and A points are independent of interaction, the positions of M and Q points are discussed in text. The stable, unstable and saddle-point FPs are denoted by large, small and underlined capital letters, respectively. See text for additional details.

functions are subleading in the scaling regime, indicating that the ladder summation is fundamentally correct in the vicinity of the stable fixed point. For attractive interaction we find that the non-universal contribution in fact changes the location of the fixed points and the values of the exponents.

We find a rich scenario of fixed points. In total there are four fixed points N, A, M, Q , but not all of them are in the physically accessible regime. Figure 4 shows the distribution of fixed points in the coupling constant $g - g_3$ plane. In each regime the stable, unstable and saddle-point (unstable) fixed points are indicated by large, small and underlined capital letters. For instance, in the case of repulsive interactions FP N describes the totally separated wires; it is the stable fixed point. FP A becomes a stable FP for strong attractive interaction. It stands for wire 3 separated from the ideal wire 1 – 2. For any attractive interaction with $g = g_3$ the FP M is stable. It corresponds to finite conductances in all ways, the value depending on the interaction strengths g, g_3 . We conjecture that M corresponds to the "mystery point" discussed in¹⁸ for the totally symmetric junction threaded by magnetic flux. The FP Q , finally, is always unstable, of the saddle point character, in the limited region where it enters the physical domain.

Most neighboring regions in Fig. 4 differ by one FP M , which appears either at the A point or at the N point, with the corresponding change in the character of this latter point. The situation at the interface between

NA and $NAMQ$ is different, as both “floating” FPs M and Q appear at one point on the parabola (see Fig. 3), away from A or N . We recall, that for equal interaction strength, $g = g_3$, the Q point appears first at $K = K_3 = 3$.

It might be also interesting to note the existence of the “tricritical” point between the phases NAM , NA and $NAMQ$, which happens at $K = 2$, $K_3 = 4/3$, (i.e., at $g = -3/5$, $g_3 = -7/25$) see Sec. IV A 3. This tricritical point corresponds to the situation when both M and Q points merge with the A point.

Comparing our findings with previous studies, we observe that there is a correspondence between the scaling exponents γ_3 in our Eq. (36) and $(1 - K_3^{-1})$ for b' in (47), and those numerically obtained by fRG method in¹⁷, respectively $\gamma_2(3)$ in Eq. (56) and $\gamma_1^{\text{HF}}(3)$ in Eq. (48) there.

We confirm that the exponents obtained by our method around N point, Eqs. (46), and A point, (47), at $K_3 = K$, coincide with those obtained by bosonization in¹⁸, Eq. (10.23), and Eqs. (10.106), (10.107), respectively. At the same time, the exponent $(1 - K^{-1})$ around the N point both in our work and Ref. [18] differs from the exponent $1 - (3K)^{-1}$ reported in Eq. (2.11) of Ref. [3] ; we note that in the latter case the RG flow exists even in the absence of interaction, $K = 1$. It was argued in^{3,18} that the bosonic theory of the Y-junction has the duality property $K \rightarrow 3/K$, which corresponds to a change from the case of totally separated wires (N point) to the case of maximally open Y-junction (D point). At the latter the conductance exceeds the value allowed by the unitarity of the single-particle S-matrix, as argued there possibly due to the formation of Cooper pairs at strong attraction. The scaling dimension of the leading perturbation around this hypothetical D point was thus found as $K/3$, in Eq. (10.30) of¹⁸, and as $K/9$ in Eq. (3.3) of³, the latter value evidently arising due to the above additional factor $1/3$ around the N point. As a result, bosonization studies predict a qualitative change in the scaling behavior of the system at $K > 3$,¹⁸ or at $K > 9$.³ Our analysis also shows a qualitative change at $K = K_3 > 3$, which corresponds to the appearance of extra FPs, but not of the exotic D type. We stress again, that the RG flows in our study always end at the surface of the (generally four-dimensional) body describing the conductance matrix in the absence of interaction. Particularly, the D point (which is $a = b = -1$ or $G_a = 1$, $G_b = 4/3$ in our notation, see²⁶) is not a fixed point of Eqs. (41) and the RG trajectories do not end there, even if we start from outside this body. Our above analysis of the three loop RG contributions confirms this picture. We have looked for contributions violating the unitarity condition as proposed in¹⁸, but did not find any. In our formalism such contributions would be generated by vertex corrections. However, at $T = 0$, all vertex corrections vanish in the d.c. limit.

In summary, we have derived a renormalization group theory description for the two independent conductances characterizing a Y-junction of a Luttinger liquid wire

(1,2) with interaction constant K and a tunneling tip Luttinger liquid wire with interaction constant K_3 . We summed up infinite classes of contributions in perturbation theory (ladder approximation) to obtain the RG β -functions. Additional contributions appearing in third order were employed to decide whether the result of the ladder approximation in the neighborhood of the stable fixed points remained unchanged. This was found to be the case for repulsive interaction (where arguments can be made that all higher order non-ladder terms should also be negligible). In the case of attractive interaction non-ladder contributions might change the critical behavior in certain cases. The existence of further fixed points, not captured by the ladder approximation, cannot be excluded, although it is not very likely. Nonetheless, we find it remarkable that our method allows to determine a rich scenario of fixed points and RG-flows, including the crossover behavior. The corresponding conductances as a function of the scaling parameter are readily accessible.

Acknowledgments

We thank D.A. Bagrets, A.P. Dmitriev, V.Yu. Kachorovskii, A.W.W. Ludwig, I. Safi, A.G. Yashenkin for useful discussions. We are grateful to I.V. Gornyi and D.G. Polyakov for careful reading of the manuscript and valuable suggestions. The work of D.A. was supported by the German-Israeli Foundation, the DFG-Center for Functional Nanostructures, and the Dynasty foundation, RFBR grant 09-02-00229. The work of P.W. was supported by the DFG-Center for Functional Nanostructures.

Appendix A: Generators of SU(3) group

For reader’s convenience, we list here the matrices λ_j used in the main part of the paper. The traceless Gell-Mann matrices, λ_j , with $j = 1, \dots, 8$ are the generators of the SU(3) group, discussed, e.g., in³⁰.

$$\begin{aligned}
 \lambda_1 &= \begin{pmatrix} 0 & 1 & 0 \\ 1 & 0 & 0 \\ 0 & 0 & 0 \end{pmatrix}, & \lambda_2 &= \begin{pmatrix} 0 & -i & 0 \\ i & 0 & 0 \\ 0 & 0 & 0 \end{pmatrix}, \\
 \lambda_3 &= \begin{pmatrix} 1 & 0 & 0 \\ 0 & -1 & 0 \\ 0 & 0 & 0 \end{pmatrix}, & \lambda_4 &= \begin{pmatrix} 0 & 0 & 1 \\ 0 & 0 & 0 \\ 1 & 0 & 0 \end{pmatrix}, \\
 \lambda_5 &= \begin{pmatrix} 0 & 0 & -i \\ 0 & 0 & 0 \\ i & 0 & 0 \end{pmatrix}, & \lambda_6 &= \begin{pmatrix} 0 & 0 & 0 \\ 0 & 0 & 1 \\ 0 & 1 & 0 \end{pmatrix}, \\
 \lambda_7 &= \begin{pmatrix} 0 & 0 & 0 \\ 0 & 0 & -i \\ 0 & i & 0 \end{pmatrix}, & \lambda_8 &= \frac{1}{\sqrt{3}} \begin{pmatrix} 1 & 0 & 0 \\ 0 & 1 & 0 \\ 0 & 0 & -2 \end{pmatrix}
 \end{aligned} \tag{A1}$$

Together with the unit matrix λ_0 , they have the property $Tr[\lambda_j \lambda_k] = 2\delta_{jk}$, with $j, k = 0, \dots, 8$. After this

normalization, the structure of algebra is determined by the structure constants f_{ijk} according to $[\lambda_j, \lambda_k] = 2i \sum_l f_{jkl} \lambda_l$. In the familiar case of SU(2) algebra (which is a subalgebra of SU(3), spanned by $\lambda_{1,2,3}$), one has $f_{jkl} = \epsilon_{jkl}$, with totally antisymmetric tensor; it leads to simple mnemonic rules. For the present SU(3) case such simple rules are absent, and in most cases we resorted to symbolic computer calculations, which are readily done, e.g., in *Mathematica*.

Appendix B: β_3 for the general Y-junction

The perturbative calculation of the corrections to the conductances, as described above, eventually leads to RG β -functions containing one-loop and three-loop contributions. The one-loop contributions are resummed into expressions (43), and the three-loop contributions to $da/d\Lambda$, $db/d\Lambda$ are found as functions of a , b , Eq. (40).

$$\begin{aligned} \beta_{3a} &= g^3 (F_2 b_2 + F_3 b_3 + F_4 b_4), \\ \beta_{3b} &= g^3 (F'_2 b_2 + F'_3 b_3 + F'_4 b_4) \end{aligned} \quad (\text{B1})$$

where

$$\begin{aligned} F_2 &= \frac{1}{864} (-432a^4 - 36a^3(b-1)\kappa + a^2(-24b^2\kappa^2 \\ &\quad + b(39\kappa^2 + 405) - 15\kappa^2 + 459) - 4a\kappa(2b^3\kappa^2 \\ &\quad - 3b^2\kappa^2 - 9b + \kappa^2 + 9) + 3(4b^3\kappa^2 - b^2(5\kappa^2 \\ &\quad + 27) + b(\kappa^2 - 81) - 36), \\ F_3 &= \frac{1-b}{288} (a^2 - b)(6(a+1)\kappa - (2b+1)\kappa^2 - 9), \\ F_4 &= \frac{1}{432} (-108a^4 - 18a^3(b-1)\kappa - 3a^2(b^2\kappa^2 \\ &\quad - 2b(\kappa^2 + 18) + \kappa^2 - 36) - a\kappa(2b^3\kappa^2 \\ &\quad - 3b^2(\kappa^2 + 3) + \kappa^2 + 9) - 27(b+1)^2). \end{aligned} \quad (\text{B2})$$

$$\begin{aligned} F'_2 &= -\frac{1}{864} (b-1)(216a^3 + 72a^2(b-1)\kappa \\ &\quad + 3a(4b^2\kappa^2 + b(\kappa^2 - 45) - 5\kappa^2 - 27) \\ &\quad + 4(b-1)(2b+1)^2\kappa^3), \\ F'_3 &= \frac{1}{288} a(b-1)^2(6(a+1)\kappa - (2b+1)\kappa^2 - 9), \\ F'_4 &= \frac{1-b}{432} (54a^3 + 9a^2(b-1)\kappa + 3a(2b^2\kappa^2 \\ &\quad - b(\kappa^2 + 9) - \kappa^2 - 9) + (b-1)(2b+1)^2\kappa^3), \end{aligned} \quad (\text{B3})$$

and $\kappa = 1 + 2g_3/g$. These expressions are used for the analysis of the fixed point M in Sec. V C. In order to compare to the result of the simple tunneling case, Eq. (52), and to our previous work, it is more convenient to go now from the "conductances" a, b to the angular quantities θ, ψ and discuss three-loop contributions to $d\theta/d\Lambda$ and $d\psi/d\Lambda$, which we denote by $\beta_{3\theta}$ and $\beta_{3\psi}$, respectively.

$$\begin{aligned} \beta_{3\theta} &= g^3 \sin \theta \sin^2 \psi \cos \psi \frac{2b_2 + b_4}{16} \\ &\quad + \frac{g^3}{128} \sin^3 \theta (f_2 b_2 + f_3 b_3 + f_4 b_4), \end{aligned} \quad (\text{B4})$$

$$\begin{aligned} \beta_{3\psi} &= g^3 \sin^3 \psi \cos \theta \frac{2b_2 + b_4}{4} \\ &\quad + \frac{g^3}{128} \sin \psi \sin^2 \theta (f'_2 b_2 + f'_3 b_3 + f'_4 b_4) \end{aligned} \quad (\text{B5})$$

with the functions

$$\begin{aligned} f_2 &= 4\kappa \cos \theta (2 \cos^2 \psi + \kappa^2 \cos^2 \theta) \\ &\quad + \cos \psi (8 \cos 2\psi - 7 + \kappa^2 (2 + \cos 2\theta)) \\ f_3 &= \cos \psi (3 - 2\kappa (1 + \cos \theta \cos \psi) + \kappa^2 \cos^2 \theta) \\ f_4 &= 2\kappa \cos \theta (\cos^2 \psi + \kappa^2 \cos^2 \theta \\ &\quad + \kappa \cos \theta \cos \psi) + 2 \cos 3\psi \end{aligned} \quad (\text{B6})$$

and

$$\begin{aligned} f'_2 &= \frac{3 \cos^2 \theta - 1}{\cos \theta} (\kappa^2 \cos 2\theta - 1) \\ &\quad + 8\kappa \cos \psi + 24 \cos \theta \cos 2\psi \\ f'_3 &= \frac{1 - 3 \cos^2 \theta}{\cos \theta} (3 - 2\kappa + \kappa^2 \cos^2 \theta \\ &\quad - 2\kappa \cos \theta \cos \psi) \\ f'_4 &= 2 \frac{1 - 3 \cos^2 \theta}{\cos \theta} + 12 \cos \theta \cos 2\psi \\ &\quad + 2\kappa (1 + 3 \cos^2 \theta) \cos \psi \end{aligned} \quad (\text{B7})$$

The previously considered case of impurity in the Luttinger liquid¹⁹ corresponds to setting $\theta = 0$ in the above equations. From the form of (B5) and Eq. (39) one verifies that the scaling exponents at the RG fixed points N ($\theta = 0, \psi = 0$) and A ($\theta = \pi, \psi = 0$) are not modified by the presence of $\beta_{3\theta}, \beta_{3\psi}$, as the latter functions contain higher powers of θ, ψ in those points.

Appendix C: Fixed point M in asymmetric case

In this section we consider the position of the FP M in case when all three bulk interaction terms g_j in Eq. (2) are different. We restrict ourselves by the first order in g_j , and use the precursor to the RG equation (37) in its general form

$$S^{-1} \cdot S_r - 1 = -\frac{1}{2} \Lambda \sum_{j=1}^3 g_j [\tilde{\rho}_j, \rho_j]. \quad (\text{C1})$$

We parametrize²⁶ the S -matrix in T -symmetric case by

$$S = e^{i\lambda_2 \xi / 2} e^{i\lambda_3 (\pi - \psi) / 2} e^{i\lambda_5 \theta} e^{i\lambda_2 \xi / 2}. \quad (\text{C2})$$

The conductance matrix in (18) is then given by

$$\begin{aligned} G_{aa} &= \frac{1}{2} \sin^2 \xi (1 - \cos \theta \cos \psi) + \frac{1}{4} \cos^2 \xi \sin^2 \theta, \\ G_{ab} &= G_{ba} = \cos \xi \sin^2 \theta, \quad G_{bb} = \sin^2 \theta. \end{aligned} \quad (\text{C3})$$

so that the Eq. (19) is restored at $\xi = \pi/2$.

Simple calculations show that r.h.s. of (C1) is zero at N fixed point, $\theta = 0$, $\psi = 0$, and at three A points : i) $\theta = \pi$, $\psi = 0$, $\xi = \pi/2$, considered above, ii) $\theta = \pi/2$,

$\xi = 0$, iii) $\theta = \pi/2$, $\xi = \pi$. The position of M point is defined by conditions $\psi = 0$ and

$$\begin{aligned} \cos \theta &= -g_3^{-1} / (g_1^{-1} + g_2^{-1} + g_3^{-1}), \\ \cos \xi &= (g_2^{-1} - g_1^{-1}) / (g_1^{-1} + g_2^{-1} + 2g_3^{-1}), \end{aligned} \quad (\text{C4})$$

at $g_1 = g_2 = g$ we return to the formulas in main part of the paper, $\psi = 0$, $\xi = \pi/2$, and $\cos \theta$ defined by Eq. (25).

-
- ¹ M. Bockrath, D. H. Cobden, J. Lu, A. G. Rinzler, R. E. Smalley, L. Balents, and P. L. McEuen, *Nature* **397**, 598 (1999).
- ² Z. Yao, H. W. C. Postma, L. Balents, and C. Dekker, *Nature* **402**, 273 (1999).
- ³ C. Nayak, M. P. A. Fisher, A. W. W. Ludwig, and H. H. Lin, *Phys. Rev. B* **59**, 15694 (1999).
- ⁴ I. Safi, P. Devillard, and T. Martin, *Phys. Rev. Lett.* **86**, 4628 (2001).
- ⁵ H. Yi, *Phys. Rev. B* **65**, 195101 (2002).
- ⁶ S. Lal, S. Rao, and D. Sen, *Phys. Rev. B* **66**, 165327 (2002).
- ⁷ S. Chen, B. Trauzettel, and R. Egger, *Phys. Rev. Lett.* **89**, 226404 (2002).
- ⁸ J. E. Moore and X.-G. Wen, *Phys. Rev. B* **66**, 115305 (2002).
- ⁹ C. Chamon, M. Oshikawa, and I. Affleck, *Phys. Rev. Lett.* **91**, 206403 (2003).
- ¹⁰ K.-V. Pham, F. Piéchon, K.-I. Imura, and P. Lederer, *Phys. Rev. B* **68**, 205110 (2003).
- ¹¹ R. Egger, B. Trauzettel, S. Chen, and F. Siano, *New Journal of Physics* **5**, 117 (2003).
- ¹² E.-A. Kim, S. Vishveshwara, and E. Fradkin, *Phys. Rev. Lett.* **93**, 266803 (2004).
- ¹³ S. Rao and D. Sen, *Phys. Rev. B* **70**, 195115 (2004).
- ¹⁴ K. Kazymyrenko and B. Douçot, *Phys. Rev. B* **71**, 075110 (2005).
- ¹⁵ T. Enss, V. Meden, S. Andergassen, X. Barnabé-Thériault, W. Metzner, and K. Schönhammer, *Phys. Rev. B* **71**, 155401 (2005).
- ¹⁶ X. Barnabé-Thériault, A. Sedeki, V. Meden, and K. Schönhammer, *Phys. Rev. Lett.* **94**, 136405 (2005).
- ¹⁷ X. Barnabé-Thériault, A. Sedeki, V. Meden, and K. Schönhammer, *Phys. Rev. B* **71**, 205327 (2005).
- ¹⁸ M. Oshikawa, C. Chamon, and I. Affleck, *J. Stat. Mech.* **2006**, P02008 (2006).
- ¹⁹ D. N. Aristov and P. Wölfle, *Phys. Rev. B* **80**, 045109 (2009).
- ²⁰ D. Yue, L. I. Glazman, and K. A. Matveev, *Phys. Rev. B* **49**, 1966 (1994).
- ²¹ S. Das, S. Rao, and D. Sen, *Phys. Rev. B* **70**, 085318 (2004).
- ²² D. N. Aristov, A. P. Dmitriev, I. V. Gornyi, V. Y. Kachorovskii, D. G. Polyakov, and P. Wölfle, *Phys. Rev. Lett.* **105**, 266404 (2010).
- ²³ I. Affleck and A. W. W. Ludwig, *Nuclear Physics B* **360**, 641 (1991).
- ²⁴ M. Fabrizio and A. O. Gogolin, *Phys. Rev. B* **51**, 17827 (1995).
- ²⁵ I. Safi and H. J. Schulz, *Phys. Rev. B* **52**, R17040 (1995).
- ²⁶ D. N. Aristov, *Phys. Rev. B* **83**, 115446 (2011).
- ²⁷ I. Bengtsson, Å. Ericsson, M. Kuś, W. Tadej, and K. Życzkowski, *Commun. Math. Phys.* **259**, 307 (2005).
- ²⁸ C. L. Kane and M. P. A. Fisher, *Phys. Rev. B* **46**, 15233 (1992).
- ²⁹ D. N. Aristov, *Phys. Rev. B* **76**, 085327 (2007).
- ³⁰ T. Tilma and E. C. G. Sudarshan, *Journal of Physics A: Mathematical and General* **35**, 10467 (2002).
- ³¹ The definition of b_4 after Eq. (49) in [19] has a wrong sign, it should read $(2 \ln 2 - 2)$ and $(4 \ln 2 - 2)$ for $T = 0$ and $T \neq 0$, respectively.